UPPSALA
UNIVERSITET

Digital Comprehensive Summaries of Uppsala Dissertations from the Faculty of Science and Technology 1687

Microfluidics at High Pressures

Understanding, Sensing, and Control

MARTIN ANDERSSON

ACTA
UNIVERSITATIS
UPSALIENSIS
UPPSALA
2018

ISSN 1651-6214
ISBN 978-91-513-0372-7
urn:nbn:se:uu:diva-353964

Dissertation presented at Uppsala University to be publicly examined in Polhemsalen, Ångströmlaboratoriet, Lägerhyddsvägen 1, Uppsala, Friday, 14 September 2018 at 13:00 for the degree of Doctor of Philosophy. The examination will be conducted in English. Faculty examiner: Professor Cyril Aymonier (CNRS, Institut de Chimie de la Matière Condensée de Bordeaux).

Abstract
Andersson, M. 2018. Microfluidics at High Pressures. Understanding, Sensing, and Control. *Digital Comprehensive Summaries of Uppsala Dissertations from the Faculty of Science and Technology* 1687. 60 pp. Uppsala: Acta Universitatis Upsaliensis. ISBN 978-91-513-0372-7.

This thesis explores understanding, sensing, and control in high-pressure microfluidics. The high-pressure regime allows fluids to be forced through narrow channels at substantial speed and creates conditions for fluids of high density and low viscosity—features desired in flow-based chemical analyses. With changes to pressure and temperature, fluid properties vary, and for miniaturized flow systems, sensing and control are needed.

For miniaturized chemical analytics to utilize high-pressure fluids, like supercritical CO_2, sensors are required for flow characterization. In this thesis, high-pressure tolerant sensors in glass chips have been developed and investigated. By the use of chip-integrated temperature, flow, and relative permittivity sensors, the variable behavior of supercritical CO_2 or binary component CO_2-alcohol mixtures have been investigated. To be able to change flow rates, a heat-based actuator chip has been developed. By a flow control system, which combines a relative permittivity sensor and heat actuated flow regulators on a modular system, the composition of binary component CO_2-alcohol mixtures can be tuned and controlled with feedback.

Flows of multiphase CO_2-H_2O hold promise for miniaturized extraction systems. In this thesis, parallel multiphase CO_2-H_2O flow has been studied. To achieve control, methods have been investigated where channels have been modified by the introduction of a guiding ridge and altered by a chemical coating. Flow is a dynamic process, where pressure and temperature can vary with time and place. As the properties of fluids containing CO_2 may change with pressure and temperature, properties will also change with time and place. Because of this, instruments with spatial and temporal resolution are needed to better understand dynamic chemical effects at flow. In this thesis, a tool is presented to study the dynamic acidification of aqueous solutions that come in contact with flowing CO_2.

By a study performed to understand the strength and pressure tolerance of glass chips, it has been found that the fracture is not only determined by the applied pressure, but also on time and environment.

Keywords: High-pressure microfluidics, supercritical CO2, compressible flow, relative permittivity, integrated electrodes

Martin Andersson, Department of Engineering Sciences, Microsystems Technology, 516, Uppsala University, SE-751 20 Uppsala, Sweden.

ISSN 1651-6214
ISBN 978-91-513-0372-7
urn:nbn:se:uu:diva-353964 (http://urn.kb.se/resolve?urn=urn:nbn:se:uu:diva-353964)

“盖有不知而作之者,我无是也。多闻,择其善者而从之;多见而识之;知之次也。”

“There may be those who act without knowing why. I do not do so. Hearing much and selecting what is good and following it; seeing much and keeping it in memory: this is the second style of knowledge.”

– **Confucius**

List of Papers

This thesis is based on the following papers, which are referred to in the text by their Roman numerals.

I **Andersson, M**., Hjort, K., Klintberg, L. (2016) Fracture strength of glass chips for high-pressure microfluidics. *Journal of Micromechanics and Microengineering*, 26(9):095009

II Knaust, S., **Andersson, M**., Rogeman, N., Hjort, K., Amberg, G., Klintberg, L. (2015) Influence of flow rate, temperature and pressure on multiphase flows of supercritical carbon dioxide and water using multivariate partial least square regression. *Journal of Micromechanics and Microengineering*, 25(10):105001

III Knaust, S., **Andersson, M**., Hjort, K., Klintberg, L. (2016) Influence of surface modifications and channel structure for microflows of supercritical carbon dioxide and water. *Journal of Supercritical Fluids*, 107: 649–656

IV **Andersson, M**., Ek, J., Hedman, L., Johansson, F., Sehlstedt, V., Stocklassa, J., Snögren, P., Pettersson, V., Larsson, J., Vizuete, O., Hjort, K., Klintberg, L. (2016) Thin film metal sensors in fusion bonded glass chips for high-pressure microfluidics. *Journal of Micromechanics and Microengineering*, 27(1):015018

V **Andersson, M**., Wilson, A., Hjort, K., Klintberg, L. A microfluidic relative permittivity sensor for feedback control of carbon dioxide expanded liquid flows, *Submitted*

VI **Andersson, M**., Svensson, K., Klintberg, L., Hjort, K., A microfluidic control board for high-pressure flow, composition, and relative permittivity, *Submitted*

VII **Andersson, M**., Rodriguez-Meizoso, I., Turner, C., Hjort, K., Klintberg, L. (2018) Dynamic pH determination at high pressure of aqueous additive mixtures in contact with dense CO_2. *Journal of Supercritical Fluids*, 136: 95-101

Reprints were made with permission from the respective publishers.

Author's contribution to the publications

I	Major part of planning, experimental and analysis.
II	Part of planning, experimental and analysis.
III	Major part of planning, part of experimental and half of analysis.
IV	Major part of planning, experimental and analysis.
V	Major part of planning, experimental and analysis.
VI	Major part of planning, experimental and analysis.
VII	Major part of planning, experimental and analysis.

Errata

Paper I – In Figure 1, the drawing of design 1 and 2 are in opposite place and, therefore, design 2 correspond to figure 1a and design 1 to figure 1b. The dimensional lengths are in their correct position.

Paper IV – The calculation of power is incorrect. Refer to the measured currents as stated in the paper.

Contents

Abbreviations

HPLC	High-performance liquid chromatography
SFC	Supercritical fluid chromatography
VLE	Vapor-liquid equilibrium
CXL	CO_2-expanded liquids
VIS	Visual wavelengths
NIR	Near-infrared wavelengths
EOS	Equation of state
BPR	Backpressure regulator
PDMS	Polydimethylsiloxane

Introduction

With the onset of the information age, most aspects of modern life are surrounded by the gathering, generation and acting on data. A great deal of such data is generated by chemical analysis, where people use it to try to figure out everything from how well a medication works to how much profit an oil reserve can give. With the ever-increasing need to generate more information, the availability of chemical analysis methods becomes highly important. This is a broader long-term reason in making this thesis. To make an analysis more available, and preferably without losing performance, scientists and engineers can improve on the necessary equipment in a few different ways: making the equipment smaller, so that it fits in your pocket; making it simpler, so that it's easier to fabricate; making it work faster, so that you can let it do more for its money; and making it more robust, so that it works wherever.

The use of small flows of liquids, gases or something which is in-between the first two (*i.e.* supercritical fluids, see later in the text) is common in many branches of analytical technology. Today, microflows—which typically is a flow which can pass in μm-scaled channels—are used in high-efficiency analyses of cells [1], genes [2] and chemical compounds [3,4]. While the science and engineering behind creating complex flow devices which utilize such small flows is an active research field, with many emerging applications, use of small flows to perform analytical tasks date back to the nineteen-sixties [5]. Back then, methods of separating analytes by a liquid flow over a column were greatly improved as high-pressure pumps started to be used to drive the liquid flow over μm-scaled particles in packed beds.

In modern times, the method high performance—or high pressure—liquid chromatography (HPLC) forms the backbone of quantitative chemical analysis in the pharmaceutical industry [6]. Together with its related technologies, it is a central tool in both investigating and monitoring environmental pollutants and food safety. By turning to a high-pressure flow, two features of great significance are enabled: one is in driving high flow rates, and the other is in using fluids with special properties only found when pressure and temperature is increased. In the first case, it can simply be noted that a flow rate can be increased by an increase in pressure, allowing for either a higher fluid throughput or for fluid to pass through increasingly tighter channels or pores. In the second case, as gases are compressed and heated, they reach conditions with

favorable fluid parameters. Carbon dioxide (CO_2) is often used for this purpose and at the proper conditions (above 30.9 °C and 73.8 bar [7]) it enters a supercritical state where it has both a gas-like and liquid-like fluid behavior.

Supercritical CO_2 can be dense enough to act as a solvent for many organic compounds and in the same time have a viscosity about a 1/10 of common solvents like ethanol. To make functional systems, applications are however dependent on a lot of equipment and knowledge. To gain knowledge and understanding, measurement tools must be developed. The ability to control and manipulate highly pressurized microflows are of great value, and if systems could be simplified and miniaturized, routes are open for increased availability of analytics. Therefore, this thesis explores the topic of flow control for high-pressure microflows, using a miniaturized system.

The miniaturization of flow devices is widespread in fields, like analytical chemistry and life-sciences, and can be summarised as microfluidics. In it, fluidic manipulation and control at the µm-scale are made, achieving benefits from small footprints, ease of integration of sensors, low dead-volumes, low material use, high thermal control and extended optical access. Working with similar technologies as microsystem technology, integration of electronics is relatively straightforward. As systems can be based on fluidic chips—rather than capillaries and wells—modular designs and the combinations of components become more accessible, taking advantages from the electronic counterpart: the printed circuit board. These advantages include system robustness and automated assembly. For flow manipulation and control, much has been done in microfluidics. Examples relying on valves [8–10] and controlled flow behaviour with wettability [11–14] are plentiful.

However, when fluids need to be contained at a high pressure, microfluidics faces challenges. A limiting factor in containing a fluid at high pressure is the strength of the components. High-end analytical fluidic systems can reach pressures around 1000 bar, putting considerable forces on components [15]. This sets requirement on designs and materials. In microsystem technology, most common materials and designs do not meet this requirement today, as the structural integrity of chip fail and components break. It is therefore important to understand the dynamics of such fractures, in order to find ways of making them stronger. Alternatively, one can also explore routes to evade too high requirements on pressure by use of binary component CO_2 mixtures (*e.g.* CO_2-expanded liquids (CXLs) [16]), which share some of the aspects of supercritical CO_2 but at lower pressures. For example, alcohols (like methanol or ethanol) show significant volume expansion when mixed with CO_2 above 60 bar and 40°C [16].

In this thesis, sensing, control and understanding of high-pressure microflows at a miniaturized scale are explored. By miniaturizing and providing means of integrated flow control components, control of both microfluidics and small-scale chromatography for chemical analysis becomes possible. In Paper I, the strength of glass based microfluidic chips and what governs pressure tolerance was explored. In Paper II and III, the focus was instead changed to better understand how highly pressured multiphase fluids behave in microflows and how their flow behaviour could be controlled. In Paper IV, high-pressure tolerant sensors in glass chips were developed, with the aim of both better understanding how the fluids behave and how to find means of controlling them in a miniaturized environment. In Paper V and VI, flow control of binary component mixtures between CO_2 and alcohols, *i.e.* CXLs, were introduced. In Paper VII, a fast measurement system was demonstrated, showing how high-pressure microfluidics can be used as a tool for better understanding high-pressure fluids and which requirements are present when miniaturizing chromatography.

Background of high pressure microfluidics

Scaling and pressure

While pressure is encountered essentially everywhere in technology, it might be a unit of measurement that is less tangible and slightly more difficult to comprehend than some other units, say the length. So, how much is 80 bar? A comparison could be made: it is about the same pressure which a diver experiences 783 m below the sea. Or, as pressure equals the applied force per area (*i.e.* P = F/A), it is like putting 5,000 kg on top of an averaged sized apple.

In microsystems, scaling laws are important as they provide means of understanding how effects changes as dimensions are altered. The force, applied by pressure, scales with a characteristic length to the second power, *i.e.* $F \propto PL^2$. For miniaturization, this has advantageous implications. Consider two round lids, one which makes up the end for a steam boiler and one which forms the top of a round cavity in a microfluidic component, the first with a radius of 25 cm and the second with a radius of 25 µm. If both the boiler and the microfluidic component are to contain 80 bar, in the first case, the lid must handle a force equivalent of 160,000 kg, in the second, only 1.6 g. This is a part of the answer to why a lid of a typical high-pressure steam boiler is made from about 10 cm thick steel while a high-pressure microchip can be made from 2 mm thick glass. Miniaturized systems, therefore, offer a way to contain fluids at high pressures using significantly less structural material than what is needed at normal, cm-length, scales.

Another aspect of miniaturizing high-pressure fluid is the contained energy. Energy densities in compressed air energy storage systems can reach between 0.5-25 kWh/m^3 [17]. In 1 m^3 of air, at 80 bar, there is roughly 7.5 kWh of potential energy stored, corresponding to the explosive power of 5.8 kg of trinitrotoluene (TNT)—a sizable explosion. However, for a microchip having storage volumes in the µL-scale, the potential energy of compressed air of the same pressure would be less than the energy content of a can of sugar-free soda.

Overall—by scaling—miniaturization is a tool for the exploration and use of high-pressure fluids, lessening the requirements on heavy equipment and creating conditions where high pressures can be explored without risk of safety.

High pressure microfluidics

For the vast majority of applications and research which has been done in microfluidics, fluid pressure is generally near atmospheric pressure and fluids are generally non-compressible, as the use of aqueous solutions and organic solvents is the most common. Though, several disciplines have found uses of miniaturized high-pressure flow and employed microfluidic technologies. Three areas are especially notable: chemical analysis, including microchip chromatography and sample preparation; material science and the processing of nanoparticles; chemical processing, requiring tools to better understand high-pressure fluids. Also of high relevance is capillary methods, which are extensively used in flow chemistry.

A good introduction for microfluidic chemical analysis at high pressure is Agilent Technologies HPLC-Chip system [18]. Being comprised of clamped and laminated polyimide channels in a replaceable form-factor, Agilent introduced a high-pressure microfluidic component to their capillary HPLC systems in 2003 which combines a sample valve, column and electrospray unit for mass spectrometry in one chip. By the lower dead volumes achieved by this concept, rather than using tubing and external components, analysis of low volume samples has become more available, finding its use in protein analysis. Utilising glass chips, microfluidic-based HPLC [19] has been investigated by several researchers, including systems which combine on-chips separation and detection with both Raman scattering and fluorescence [20], droplet generation [21] and superheated eluents [22]. Several concepts of liquid-supercritical fluid extraction have been explored: for parallel flow, measurements of partitioning of a cobalt complex have been done [23]. For segmented flow, extractions of lignin oxidation products [24] and vanillin [14] have been done. Paper II and III are further investigations of parallel flow designs. Paper IV, V, and VI deal with control of microfluidics, which is relevant to chromatography.

For material sciences, high-pressure microfluidics has been used for the production of nanoparticles. The high thermal control and the possibility of precise residence times have allowed for the production of quantum dots with a very narrow size distribution. To increase performance, both supercritical CO_2 [25] and supercritical hexane [26] has been used. In the field of flow chemistry, where chemical reactions are done at flow, the small length scales and control of residence times offered by microfluidics allow for higher efficiency and selectivity of chemical reactions. By turning to higher pressures and temperatures, novel process regimes can be entered.

The area where most high-pressure microfluidic applications are found is in tools for better understanding of fluids at high pressures. Such tools are of high relevance for anyone whose application deals with pressurized fluids and

typical applications are found in chemical processing, *e.g.* petro-chemistry [27,28] and synthesis. Typically, such systems compete with mL-batch containers which can hold the fluids, and by use of pistons, sight glasses, and samplers; one can analyse parameters such as vapor-liquid equilibriums (VLE), solubility and partitioning. As microfluidics allows for flow analysis and multiplexing, such studies can be made faster and a lot more data can be generated. An important feature in these tools is the planar design that microfluidic chips can give, allowing for an easy-to-study optical plane and good thermal contact with temperature control units. Examples include visual phase equilibrium studies using 10,000 microwells [29], bubble and dew point detection under flow [30] and stepwise dew point measurements [31]. To study CO_2 solubility, several systems have been presented [32–34]. For determination of vapor-liquid equilibrium data in microflows, Raman spectroscopy has been used [35]. Paper V, VI, and VII are further examples of tools where microfluidic systems allow for studies of either dielectric properties or pH changes.

A large number of applications also use high-pressure microflows in tubes or capillaries—not microfluidics. In these cases, the benefits—such as higher pressure tolerance, simplicity and easy access to tubing of a wide range of material choices—can outweigh those of planar chips.

A need of instrumentation and control

In order to work with microflows at high pressure and to be able to flow compressed fluids, dedicated fluid components such as pumps, valves and regulators are needed. With its ongoing effort for higher performance, chromatography has become the main driving application for research of such components. In HPLC, with flow rates in the mL/min range, many applications demand lower sample volumes and lower solvent consumption, which has led to the development of pumps for lower (nL to low µL/min) flow rates [36]. A key aspect is to provide a flow of high stability and minimal pulsing [37]. Because of this, use of flow splitters and packed column restrictors have been employed [38]. Reciprocating pumps, a type of displacement pump, are most favoured as they allow for continuous pumping to high pressures, but other types include pneumatic and syringe pumps [36]. Reciprocating pumps deliver a pressure pulse between each stroke while syringe pumps can deliver a pulseless flow. However, syringe pumps require refilling after the internal volume is empty and, if the syringe volume is large, the compressibility of the fluid can affect flow equilibrium times. The pulsing of reciprocating pumps can be reduced by dampers and dual pistons [39]. For high-pressure microfluidics, both reciprocating and syringe pumps are used.

The technical aspects of microflows containing compressed CO_2 is best exemplified by a related technique, supercritical fluid chromatography (SFC). Being a method with a history as long as that of HPLC, the field has been struggling with flow control since its beginning [40]. A major challenge is to keep CO_2 dense, which is achieved by pumping, cooling and back-pressure regulation (BPR). To pump CO_2, or any common liquid over a large enough pressure difference, one has to take into regard the compressibility of the fluid. In essence, compressibility makes a fluid behave similar to a spring, where a reduction of the fluid volume by pressure (*e.g.* by the stroke of a displacement pump) achieves an increase in density. Flow, however, will only occur if the pressure at this reduced volume is higher than that of the downward flow system. Because of this, a lot of research effort has been put on solvent delivery systems for CO_2. First of all, to achieve a useful mass flow, a mere pressure increase is not enough; the fluid must be dense, which requires cooling. Secondly, a precisely defined flow of mixtures containing CO_2 and other solvents are often needed. To achieve this, metering of the flow is needed. In the case of negligible compressibility, this is done by knowing the number of strokes per unit of time and the volume of their displacement. An example of this is the common low-pressure syringe pumps used in microfluidics, where the linear movement and cross-section of the syringe plunger is used to define the flow rate. When a fluid is compressible, alternative methods have to be employed to adjust the flow [41]: pre-compression by booster pumps to a low compressibility condition, followed by metering the displacements in a secondary pump; adjustment of displacements by calculation of compressibility effects with an equation of state (EOS); and measurements of flow rates using mass flow meters.

For flow control, another critical aspect is that the fluid often must be kept in a dense condition further down in the flow system, requiring a back-pressure regulator. For CO_2 to be liquid, pressure over the fluid system must not drop below the vapor-liquid equilibrium, and to be supercritical not below its critical temperature and pressure. Mechanical—spring-loaded—backpressure regulators (BPR) provide a low variation of pressure at a given point over a wide flow range. However, for chromatography, requirements are higher. Control systems which measure pressures over such fluid systems and uses electrical actuators (either solenoids [42] or stepper motors [43]) to set either the open duty time [42] or the position [43] of valves in order to regulate the pressure are commonly used. When flow rate and backpressure do not need to be varied, flow restrictors (*i.e.* capillaries) can be used.

While both HPLC and SFC belong to their own discipline, the same mechanics and needs are put on high-pressure microfluidics. Precise microflow is a necessity in microfluidics and if advances of new applications are to be made

in high-pressure microfluidics, control of compressible fluids and a better understanding of high pressures microflows are needed. In this thesis, work has been put in to better understanding of what requires control and how control can be achieved when working in this environment. For miniaturization, one concept is to reduce the need for bulky moving parts, such as valves and pumps. This is explored in Paper VI, where control of the fluid composition, relative permittivity and flow rate was achieved with a microfluidic control board. Microfluidics opens up for new ways to do extractions, and for it, multiphase flow control is needed. In Paper II, a statistical analysis of different system parameters was done in order to investigate what affects multiphase parallel flow. An interesting aspect of multiphase flow control is that, at this scale, also surfaces affect the fluid behaviour — this was investigated in Paper III.

High-pressure fluids

Carbon dioxide

While CO_2 at ambient conditions, *i.e.* atmospheric pressure (1 atm) and room temperature (21 °C), is a gas, it can, by a moderate increase in pressure to 58 bar become a liquid and be used as a solvent in flow systems. To be a solvent, it has to have the ability to dissolve other compounds, giving it a solvent power. The solubility of compounds, *i.e.* the maximum concentration of a substance that can be dissolved in a phase, is affected by solute-solvent interactions, the vapor pressure and the molecular size of the solute. CO_2 has zero dipole moment, d_μ, and a low static relative permittivity, ε_r, of 1.4 (for the liquid state at 25 °C [44]) and while it often has been regarded as a non-polar solvent, it has polar attributes [45] and can, therefore, dissolve a wide range of different compounds. If temperature, T, and pressure, P, are increased further, to 31.0 °C and 73.8 bar, the critical point of the fluid is reached and it becomes supercritical. At and beyond this point, the fluid cannot be described as being either a liquid or a gas, but rather a combination of both and no VLE can be described. By transitioning from ambient conditions to well beyond the critical point, several important fluid properties of CO_2 changes. For a flow of CO_2, two properties can be considered of special importance:

- Density, ρ. By either increasing pressure or decreasing temperature, CO_2 becomes denser. The relationship between these parameters can be described by an equation of state [7]. At room temperature vapor-liquid equilibrium, CO_2 exerts a pressure of 58 bar with the liquid phase and gas phase having a density of 764 and 201 kg/m^3, respectively. Variations in density from a liquid state to supercritical conditions can be striking, *e.g.* at a constant pressure of 80 bar, transitioning from 7 to 37 °C changes the density from 923 to 328 kg/m^3, *i.e.* a 65% loss in density.
- Dynamic viscosity, μ. The transport properties of CO_2 also depend on pressure and temperature. Using models based on both theoretical models and measured data [46], viscosity can be described as a function of density and temperature.

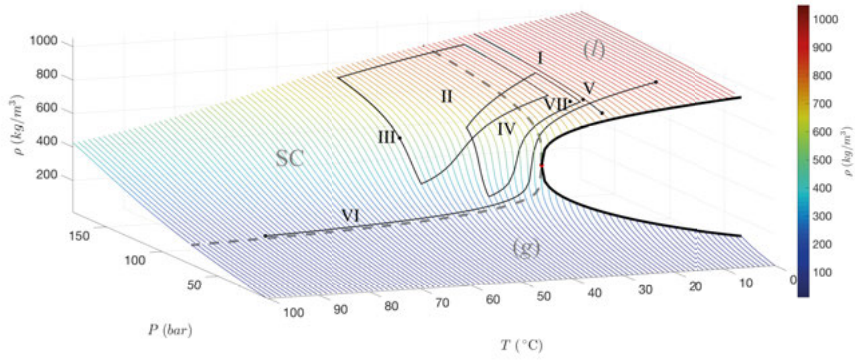

Figure 1. Density, ρ, as a function of pressure and temperature over the range 0 to 100 °C and 5 to 180 bar. In the figure, which is a 3-dimensional representation, the density is represented by both the z-axis and the color of the curves. The liquid (*l*) and gas (*g*) phases are found in high (red) and low (blue) densities regions, respectively, and are separated by the VLE (black thick curve). Supercritical conditions (SC) are found at temperatures and pressures above the critical point (red dot), at 31.0 °C and 73.8 bar, which forms a border to the supercritical region (dashed grey curve). The papers covered in this thesis are also marked at the corresponding pressures, temperatures and densities where the studies were performed. Paper II and IV explored different pressures and temperatures (black bordered regions). Paper III, VII and V were measured at specific points (black dots). In Paper I and VI, either pressures or temperatures were varied (black curves with dots at the ends). Data were calculated from the Span-Wagner equation of state [7].

Density as a function of the *P* and *T* region explored in this thesis is shown in figure 1 and provide an overview of the changes that can be expected for any CO_2 containing flow system working at different *P* and *T* conditions. Viscosity is shown in figure 4a. As an example, at 100 bar, transitioning from a cooled liquid state of 4 °C to a supercritical condition at 40 °C, lowers the density and viscosity with 34% and 50%, respectively. For a system which runs at true isobaric and isothermal conditions, variations of ρ and μ is zero. However, even a ±1°C temperature variation induces significant changes, *e.g.* these are 6% and 4%, respectively, at 40 °C and 100 bar for the density and viscosity, respectively. In SFC, pressures are typically higher, and the properties of CO_2 are more stable. For example, a temperature variation of ±1°C at 200 bar and 40°C corresponds to a density variation of about 1%.

Binary CO_2 mixtures

The solubility of compounds is set by their interaction with the surrounding solvent. For common liquid solvents, which all have high densities, the intermolecular forces between solvent and solute are an important characteristic. For fluids with densities varying from that of a gas to that of a liquid, the situation becomes more complex. Then, the melting point, or vapor-pressure, of the solute and the density of the solvent become key aspects and solubility becomes a function of pressure and temperature [47]. For many CO_2 applications, for example in processing and analysis of either pharmaceutical compounds or food products, low molecular weight organic compounds of low polarity are used which have melting points above the critical temperature of CO_2. In general, if solids of such compounds are exposed to increased pressures of CO_2, the melting point of the solids decreases [48]. For many compounds, technically relevant solvent powers are achieved at pressures where the density starts to be similar to common organic solvents—roughly above 150 bar.

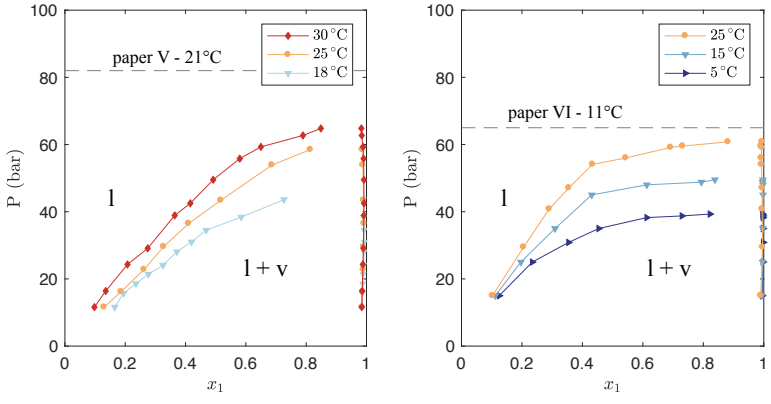

Figure 2. Pressure at the vapor-liquid equilibrium for different temperatures as a function of increasing molar fraction of CO2, x_1, for either ethanol (left) or methanol (right). The figure is generated from data belonging to C. J Chang et al. [49] and K. Bezanehtak et al. [50]. The two-phase region, containing liquid (l) and vapor (v), is seen in the lower part of the graph and the single-phase region, containing only liquid, is seen above the curves. The lower pressure limit and temperature, from which the studies in Paper V and VI were performed, is indicates (dashed grey lines).

By the introduction of a second component to CO_2, the solvent properties can be changed. If a cosolvent is added, such as methanol or ethanol, the resultant mixture can have a high density at a lower pressure. As alcohols also have higher polarity, it becomes easier to dissolve more polar compounds [51]. Depending on pressure, temperature and composition; either a single liquid phase, or a liquid phase and a vapor phase, will form. Given that either the

temperature is low or that the pressure is high, the resultant mixture is fully miscible over the entire compositional range, figure 2. In Paper V and VI, binary CO_2 mixtures containing either ethanol or methanol were used.

Binary mixtures of CO_2 and alcohols share fluid properties belonging to their pure components and they allow for an interesting combination of properties that can be tuned. For example, over the compositional range of 0 to 85% CO_2, the viscosity of CO_2-expanded methanol at 30 °C drops from 513 to 110 µPa·s [52]. Meanwhile, density only changes by less than 10%. In supercritical fluid chromatography, the CO_2 based mobile phase is often modified by additions of methanol, up to 50% [53]. Together with other additives, this allows for separations of both acidic or basic compounds of high polarity [54]. Alternatively, by introducing small amounts of CO_2 to mobile phases typically used in liquid chromatography, the fluidity of the liquid can be increased [55]. In extraction and reaction, CO_2 expanded liquids (CXL) are used. For example, by working with CO_2-ethanol fluids in extraction, extraction efficiency can be improved [56]. By precisely defining and tuning the composition of the CXL, elaborate extraction and reaction schemes can be made with increased selectivity [16].

At ambient conditions, the static relative permittivity, ε_r, of ethanol and methanol is 24.5 and 32.7, respectively [57]. ε_r is a common and useful parameter in describing the polarity of a solvent, and when mixing two very different solvents, like CO_2 and alcohols, changes are significant. For a pure component, Kirkwood theory [58] can be used to relate the polarization, φ, of a fluid per unit volume with the relative permittivity. For a pure component, this can be described as,

$$\varphi = \frac{(\varepsilon_r - 1)(2\,\varepsilon_r + 1)}{9\,\varepsilon_r} = \frac{4\pi N_A}{3V_f}\left(\alpha + \frac{d_\mu^2 g}{3k_B T}\right) \quad (1)$$

where, d_μ is the dipole moment, N_A is the Avogadro constant, α is the molecular polarizability, k_B is the Boltzmann constant and g is a correction factor. V_f is the molar volume, $V_f = M_f/\rho$, of the fluid. M_f is the corresponding molar mass. For binary component fluid mixtures consisting of the components A and B, the polarization of a mixture, φ_m, can, to a first linear approximation, be estimated by the following expression,

$$\varphi_m = \frac{xV_A\varphi_A + (1-x)V_B\varphi_B}{xV_A + (1-x)V_B}, \quad (2)$$

where φ_A, φ_B and V_A, V_B represents the polarisation and molar volumes for the two pure components. By this, there is a relationship between the molar fraction, x, of binary fluid mixtures and the relative permittivity.

Binary phase systems: CO_2 and water

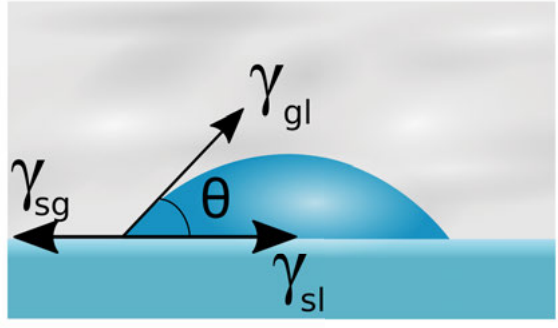

Figure 3. Drawing of a wetted drop on a surface, having a wetting angle θ. The drop, solid phase and the surround fluid each make up a phase.

CO_2 and water are immiscible and when the two components are mixed, a two-phase fluid will form. When a water drop contacts a glass surface; the CO_2, water, and glass makes up for a three-phase system. At their shared triple contact point, the three surface tensions of the glass-CO_2 (γ_{sg}), glass-water (γ_{sl}), and CO_2-water (γ_{gl}) are in equilibrium, giving and the water drop a wetting angle θ, figure 3. Their relationship can be expressed by,

$$\gamma_{sg} - \gamma_{sl} = \gamma_{gl} \cos\theta. \tag{3}$$

The wetting behaviour is pressure dependent, and on silica surfaces, which like glass is intrinsically hydrophilic, it has been noted that as CO_2 pressure increases, so does θ, giving a lower wetting ability of water on the surface, and (γ_{gl}) decreases [59]. At 100 bar, contact angles are between 15-30°, and water wets glass better than CO_2. By changing the fluids interactions with the glass, other wetting angles can be achieved. Methyl and fluorocarbon coated surfaces lead to a more hydrophobic surface, i.e. increasing γ_{sl}. Likewise, methyl and fluorocarbon groups have low intermolecular forces and can be expected to be more CO_2-filic, thereby decreasing γ_{sg}. Use of such surfaces was explored in Paper III.

While CO_2 and water are immiscible, some CO_2 is soluble in water, about 6% by weight at 100 bar and 30 °C [60]. Here, solubility increases with pressure and decreases with temperature. Similarly, some water also dissolve in CO_2 [61], which has implications for the strength of glass chips, which was discussed in Paper I.

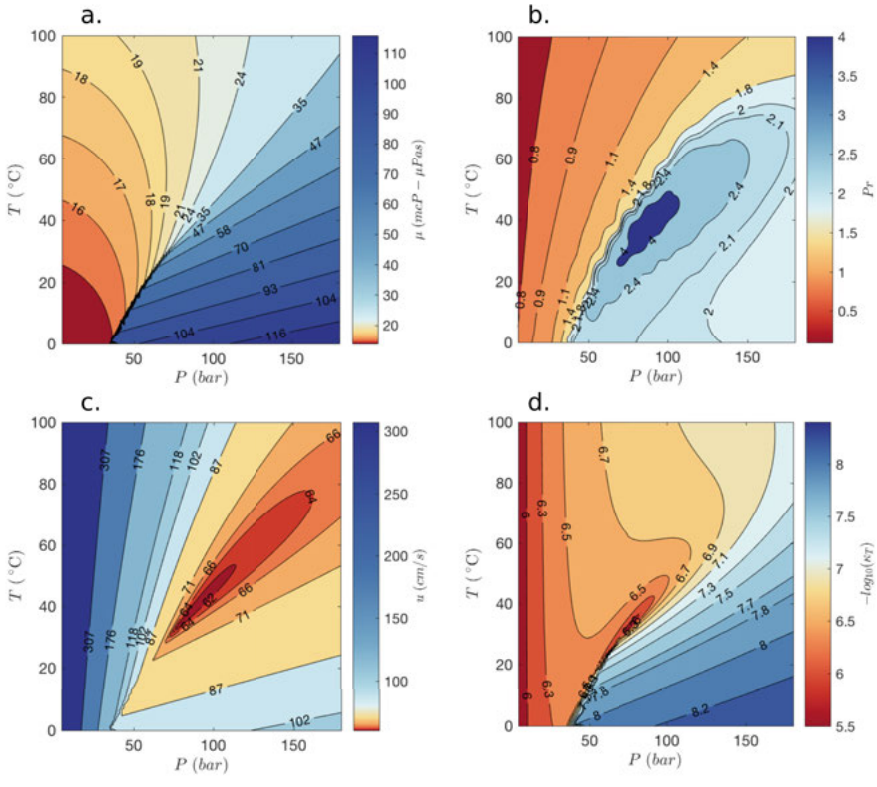

Figure 4. Contour plots relevant for microflows of CO_2 over the range 0 to 100 °C and 5 to 180 bar. (a) the viscosity, μ, decreases as the supercritical regime is entered and as the density becomes more gas-like. Data calculated from [46]. (b) the Prandtl number, *Pr*, diverges close to the critical point. Data calculated from [7,46,62]. (c) The average velocity, u, for the case of Re = 1700 and L = 200 µm over the range 0 to 100°C and 5 to 180 bar. For this length scale, typical in this thesis, flow can be considered laminar bellow these average velocities. (d) Isothermal compressibility, κ_T, expressed in the -log 10 scale for CO_2 over the same range. At liquid conditions, e.g. 20 °C and 80 bar, κ_T is 2.1×10^{-8} Pa^{-1}.

Pressure driven flow

Laminar flow with CO_2

The fluid dynamics can be described by dimensionless numbers that are useful in understanding scaling effects occurring in microflows. One number of importance in microfluidics is the Reynolds number, *Re*, which can be used to assess if the flow is turbulent or laminar. Being the ratio between inertial and viscous forces [63], it is defined as,

$$Re = \frac{\rho u L}{\mu} \tag{4}$$

where u is the velocity and L is a characteristic length scale, *e.g.* the hydraulic diameter. At low *Re*, flow is laminar, and when increased above 1700 – 2300, turbulence occur [64]. Therefore, in microfluidics with aqueous or organic liquids, with L being in the order of µm, flow is almost always laminar. However, for a high-velocity flow of dense fluids with low viscosity, this does not need to be true. In the case of CO_2 microflows, viscosity can be low while density still is comparably high, giving conditions which are closer to turbulence at the cm/s scale. The onset of turbulence occurs at lower flow rates around the critical point, figure 4c. The multiphase flows in II, III and VII have maximum estimated velocities of 25, 5 and 5 cm/s, respectively, and the flow sensor in Paper IV was characterized at flow velocities up to 8 cm/s. For those flow rates and dimensions, flow is laminar. In Paper V and VI, average velocities were locally higher, as smaller dimensions were used (*i.e.* 20 µm wide capillaries in Paper IV and either 8.7 or 16.7 µm deep channels in Paper VII) and conditions are less laminar. In Paper VI, which featured 16.7 µm deep channels, *Re* numbers were also affected by the different temperatures used, being about 200 at 8°C and higher, around 760, as the fluid reaches a critical temperature.

When conditions are laminar and the fluid can be considered incompressible, the Hagen–Poiseuille equation [65],

$$\Delta P = RQ \tag{5}$$

can be used to describe the linear relationship between the pressure drop ΔP and the volumetric flow rate, Q in channels. The restriction, R, in the channel,

$$R = \frac{8\mu L}{\pi {r_H}^4}, \tag{6}$$

is dependent on μ and the geometrical length, L, and hydraulic radius, r_H, of the channel.

Compressible flow

When CO_2 flows in channels where pressure, temperature and cross-sectional areas of channels change, the relationships between density, pressure, and temperature dictate the flow. For example, if CO_2 is pumped from a cooled piston pump, the same volumetric flow will not necessarily pass a chip further down the fluid system. Instead, one must consider the mass flow, $\dot{m}$, which stays constant throughout the fluid system,

$$\dot{m} = Q_i \rho_i, \tag{7}$$

where the index i denotes a location where both the volumetric flow rate and the density is well characterized. If the pump is kept at 5 °C and 100 bar, the density of the CO_2 in the pump is 948 kg/m^3 and a 100 µL/min flow holds a mass flow of 1.6 µg/s. For a chip held a 40 °C and pressure gradient running from 100 to 80 bar, the corresponding change in density gives a volumetric flow of 152 to 332 µL/min.

While several models used in microfluidics require an important condition: non-compressibility, the large density variability of CO_2 creates conditions were a flow can be considered compressible. For the limiting cases of either isothermal ($i = T$) or adiabatic ($i = S$) conditions, one can define the compressibility, e.g. the relative volume change of a fluid by a change in pressure, in terms of density,

$$\kappa_i = \frac{1}{\rho}\frac{d\rho}{dP} \tag{8}$$

where $\kappa_S < \kappa_T$ at these conditions. The compressibility of CO_2, figure 4d, varies by orders of magnitude over the pressure and temperature regime close to the critical point, being considerably more compressible than alcohols, *e.g.* ethanol has a κ_T of $1.1 \cdot 10^{-9}$ Pa^{-1} while the compressibility of CO_2 is higher, about $1.5 \cdot 10^{-7}$ Pa^{-1} at 40 °C and 100 bar. Therefore, the flow behaviour of CO_2

and CXLs can be non-intuitive and flow at the desired conditions become difficult to achieve. Furthermore, the Hagen-Poiseuille equation, (5), at high κ, loses validity.

During isothermal conditions, and if the flow is subsonic, the errors from approximating a compressible flow as being non-compressible can be estimated by κ_T, μ, ρ, Re and the dimensions of the channel [65]. For the flow velocities and dimensions of channel used in this thesis, such errors are less than 5% in the liquid region, but can, as the temperature is increased, reach a point where flow conditions become too compressible to describe. In Paper VI, which worked partially in this regime, a relative permittivity sensor, mounted downstream where such conditions occur, instead provided understanding of the flow conditions.

Thermal considerations during flow

With microfluidics, the short length scales do implicate better heat transfer than for larger systems and isothermal conditions in chips are typically assumed. When local heating or cooling of CO_2 occurs, changes of the viscosity and density can be expected. To better understand this process under supercritical conditions, several research groups have investigated the complex flow behaviour of CO_2, using numerical models of the combined heat and fluid dynamics [66,67]. While most real fluid-heat problems need to be addressed through means of modelling, *e.g.* using finite element methods, some heat-related quantities give valuable insight in general. The Prandtl number [68], *Pr*, is one such useful number, which gives the ratio between momentum diffusivity and thermal diffusivity,

$$Pr = \frac{\mu/\rho}{\alpha} = \frac{c_p \mu}{k}, \tag{9}$$

where α is the thermal diffusivity ($k/\rho c_p$), k is the thermal conductivity and c_p is the heat capacity at isobaric conditions. A fluid at flow form a hydrodynamic boundary layer and when the fluid passes a heated surface, a thermal boundary layer also forms. This layer controls the rate of heat flow and by *Pr*, the relative thicknesses of these two layers can be compared. *Pr* depends only on fluid specific parameters and at ambient conditions, it is stable—typically less than 1 for gases (*e.g.* 0.7 for air) and higher than 1 for liquids (*e.g.* 7.6 for water). In figure 4b, *Pr* for CO_2 around the critical point can be seen. *Pr* varies from more liquid-like to more gas-like numbers and as properties diverge around the critical point [69], *Pr* reaches a local maximum [70]. By *Pr*, one can estimate the length required to develop a thermal profile [71], and for a cm/s scaled flow of CO_2 to enter a heated section of a 25 µm wide circular

channel, about 1 mm of channel length is required when conditions stay in the liquid region. Close to the critical point, this length should be significantly longer. In both Paper IV and VI, where localised heating in channels was used, regions of variable thermal properties were entered.

Fluid models

If the dimensions are well known, as is possible with microsystem technology, then (5) can be used to estimate flow rates at static conditions. Due to the simplicity of working with linear relationships, linear equivalent circuit models can be used to understand flow when more than one flow rate and pressure must be regarded, as is the case in mixing. This concept was utilized in Paper V and VI for CO_2 binary mixtures with a variable composition of ethanol and methanol in CO_2. In Paper V, the method was used to estimate the composition of mixed flows. In Paper VI, the model was used to explain the working principle of a control system that can both tune and stabilize binary component methanol-CO_2 flows.

Multiphase flow

For multiphase flow, low velocities and small channel sizes generally favour interfacial forces over those linked to gravity, viscosity, and inertia [69]. For immiscible fluids, the flow behaviour depends on the geometry, flow rates and instabilities between interfaces of the two phases, can lead to either a segmented or a parallel flow. At cm/s-scale microflows of CO_2 and water, interfacial forces typically dominate, and rather than flowing in parallel like a laminar single phase flow would do, the surfaces between the phases can take on a minimised shape by forming segments. Segmented flow gives an orderly behaviour to the flow and was used in Paper VII. Having a flow in parallel does, however, offer some unique design opportunities as it gives a well-defined interface area from which to conduct studies of, *e.g.*, extraction. In Paper II and III, CO_2 and water were emitted from Y-junction into a shared channel and it was investigated how such a parallel flow can be achieved and what affected it. The interfacial forces are important to control and manipulate the parallel behaviour, and in Paper III, surface modifications were introduced to further control and stabilise the flow. By altering the surfaces to wet both fluids more equally, and have a wetting angle, θ, closer to 90°, stability could be improved. To further lock the interface in place, a ridge was introduced into the channel, which helped in pinning the interface in the centre of the channel.

Pressure tolerance in microsystems

Materials in high pressure microfluidics

To create microfluidic components, dependent on the application, requirements are put on the properties of the fabrication materials:

- Optical: In order to characterize a fluid flow, the ability to have optical transmission is central. The planar attribute of chips offers an ideal platform for visual studies by microscopes from which studies, *e.g.* of multiphase flows, become possible. For chemical detection of compounds by spectroscopy, the ability to pass either reflective or transmitted light, for a wide range of wavelengths, through a fluid channel is essential.
- Electrical: For many sensor principles, electrical circuitry is required which needs to be integrated into the component. This requires both electrically conducting and insulating materials.
- Thermal: For studies that require either isothermal conditions or that heat is added or removed, the thermal conductivity of the materials surrounding the flow affects the performance.
- Chemical: The materials must hold chemical resistance and must not corrode or swell. Furthermore, the material should have a low permeability to chemical compounds. Also, chemical compatibility with different fabrication materials and methods must be assured.
- Mechanical: The combination of properties such as fracture stress, fracture toughness, elasticity, plasticity and ductility of materials together form the basis for a components pressure tolerance as it affects both the overall component reliability and the ability to form bonded interfaces.

To exemplify this, one can examine a common material in microfluidics: dimethylpolysiloxane (PDMS). It is chemically resistant to a wide range of aqueous solutions, electrically insulating and have optical transmission over a wide wavelength range [72]. Before curing, the material is viscous and can conform to structured surfaces. After curing, the high elasticity allows it to conformably adhered to height variable substrates, *e.g.* to glass with conductive thin film pathways on top. Together with a few other polymer-based materials (*e.g.* acrylic, polycarbonate, and polystyrene), it is therefore ideal for

low-pressure, aqueous-based, applications found in the life sciences. Unfortunately, PDMS fail at higher pressures and is rarely used above a few bar. For applications that require higher pressures and non-aqueous fluids (*e.g.* non-polar solvents and gases), finding the ideal material is however not trivial. Components are therefore often based on non-permeable materials which do not swell by organic solvents. Three common material combinations are:

- Stainless steel. 304 type stainless steel laminates have been demonstrated with supercritical water at 250 bar and 750 °C [73]. While its non-transmittence is a hindrance in some applications, a major drawback is in its fabrication. To create joints between laminates of mechanical properties similar to the bulk materials, pressurized thermal diffusion bonding at temperatures from 850 °C is done [73]. Due to the passivated oxide film of stainless steel, these systems can have a high corrosion resistance for a wide range of solutions. The thermal conductivity of stainless steel is about 13-17 $Wm^{-1}K^{-1}$.
- Silicon-glass. Large chips (several cm in width) made from silicon and borosilicate glass have been demonstrated in continuous operation at 250 bar and 450 °C for microreactions [74]. With 200 µm wide channels, systems have been shown to handle 450 bar at room temperature. Other smaller systems have been demonstrated at 500 bar [75]. By the use of borosilicate glass, which has a high optical transmittance over the wavelength range 340 to 2250 nm, reflective light measurement can be assured in the visual range (VIS) as well as into the near-infrared wavelength (NIR) range. For corrosion resistance, silicon is also dependent on a passivating oxide film. A major advantage of using silicon is its compatibility with microsystem fabrication methods such as dry etching, giving the ability to produce high aspect ratio channels. The silicon and borosilicate glass combination further allows for use anodic bonding, a method in where a high voltage is applied over the pre-bonded wafer stack at temperatures ranging from 250-450 °C. This causes alkali ions in the glass to diffuse into the bond interface, creating a strong bond. The thermal conductivity of silicon is about 149 $Wm^{-1}K^{-1}$.
- Glass-glass. Chips which only use borosilicate glass as a structural material have been shown to sustain pressures up to 690 bar in 120 µm wide channels [76]. Similarly, to silicon-glass chips, glass-glass chips can be used in the VIS-NIR range, but as both wafers are transparent, absorbance measurements through the chips can be made. Here, corrosion resistance is not provided due to a passivating film, but instead provided by the bulk material being an inert

oxide, giving resistance against many strong acids, bases, and organic substances. Borosilicate glass is further advantageous for fabricating integrated thin films due to several reasons: it is an insulator; it does not react with common thin film materials such as Pt, Au and Ni; and at elevated temperatures, it can flow at high temperature and is therefore able to seal bond interfaces when variations in the topography is present. Anisotropic channels can be produced in borosilicate glass by dry etching, but require other methods than those used for silicon as non-volatile products, such as Na_2F, is formed in the process [77]. The thermal conductivity of borosilicate glass is about 1.2 $Wm^{-1}K^{-1}$.

It should also be mentioned that polymers have been used at high pressure. One example is glass sandwiched with UV-curable off-stoichiometry thiolene epoxy (OSTE), which have been showed to be able to sustain pressures of 200 bar [78]. Furthermore, structurally integrity can also be achieved by putting chips on an external load by clamping. By that method, high-pressure micro components have been achieved from material combinations such as parylene bonded stainless steel laminates and polyimide laminates [79].

Pressure tolerance and its relationship to materials and geometry

While stainless steel, glass, and silicon all are used in high-pressure microfluidics, their mechanical properties are different: the first being a ductile material, the others being brittle. The fracture strength of austenitic stainless steels can be described by its yield strength and tensile strength, which depending on its grade, is in the range of 286-500 MPa and 760-1280 MPa, respectively [80]. For silicon, it is more complicated. Depending on the size, production method and form of the silicon material, fractures stresses vary. For a lapped silicon wafer, the median fracture stress has been measurements to be 270-330 MPa [81]. When the strength of silicon micro components instead is evaluated—strengths can be considerably higher—such as for micro cantilevers, which can have an average fracture stress of 8.1 GPa [82]. Such large differences in fracture stress can be attributed to brittle fracture mechanics. Ductile materials, such as stainless steel, have a high resistance to brittle fracture in presences of a crack, *i.e.* a high fracture toughness, K_{ic}, while brittle materials, such as silicon and glass, are more sensitive to brittle fractures in presence of a crack. For stainless steel, K_{ic}, is 112-278 MPa $\cdot$ $m^{1/2}$, while for glass and silicon, it is considerably less, typically between 0.7-1.3 [83] and 0.6-0.8 MPa $\cdot$ $m^{1/2}$ [84], respectively.

Thus, while glass and silicon are theoretically materials of high strength, they are considerably more sensitive for cracks, *i.e.* defects, in and on the material. The geometry dependent distribution, size and number of defects therefore influences the fracture stress of brittle materials. Consequently, defects are important for understanding the pressure tolerance of chips. While bulk defects, intrinsic to the material, have one effect, surface defects in the microfluidic channels are also present. Typically, they are the result of the fabrication and can be related to bonding and etching. For bonding, chemical pre-treatments and unevenness between bonded substrates produce different conditions at the bond interface compared to the bulk. Therefore, it is likely that this interface constitutes a region where cracks more easily can be initiated. Moreover, as the defects have a random occurrence and size, also pressure tolerance has an element of randomness—leading to some chips having a higher strength than others. To make matters even more complex, cracks can grow and develop over time. At the moment a fracture occurs, the combination of stress and crack size reaches a critical limit. This limit can be reached either by an increase of stress (through an increase of pressure) or, by an increase of crack size. One mechanism behind crack growth is environmental stress corrosion. The corrosion, which has been identified in both glass and silicon (through its passivating surface oxide, SiO_2), is believed to occur due to the stress stretching the chemical bonds of the material which then more easily react with compounds, such as water, in the surrounding environment. Because of this, the strength of chips becomes a function of several variables: stress, temperature, time and environment. Consequently, the measured fracture toughness of glass chips done in Paper I, about 0.31-0.58 $\mathrm{MPa} \cdot \mathrm{m}^{1/2}$, were considerably lower than what is found in pure material tests (*i.e.* 0.7-1.3 $\mathrm{MPa} \cdot \mathrm{m}^{1/2}$).

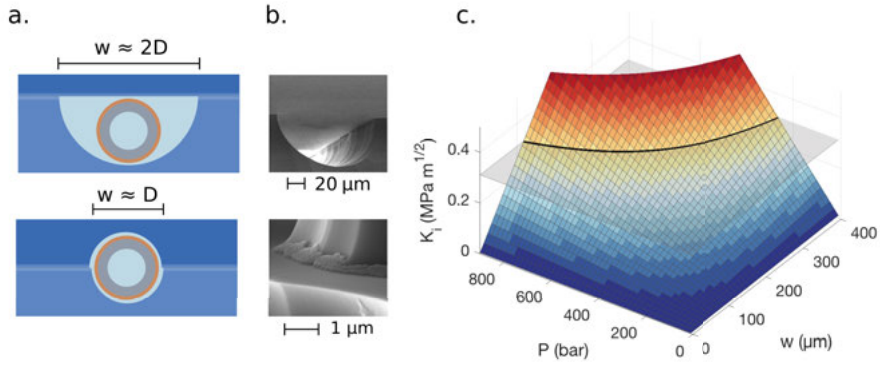

Figure 5. (a) Drawing of cross-section for two types of channels (light blue) with a capillary (grey and orange) inserted into it. (top) Semi-circular channel formed by etching one wafer isotopically and bonding a flat lid on top. To fit a capillary of outer diameter D, a channel width, *w*, of more than 2D is required. (Bottom) Channel formed by isotopic etching of two wafers which are aligned and bonded to form a circular cross-section. A small misalignment is indicated in the figure. (b) Two images taken by a scanning electron microscope together with scale bars: (top) a semi-circular channel showing both the flat and etched wafers; (bottom) the misalignment between two etched wafers, showing the flat un-etched surface of one of the wafers in the middle, and the etched sides at both the top and bottom. (c) Graph showing the relationship between pressure, *P*, channel width, *w*, and estimated stress intensity factor, K_i, for a channel. As K_i exceeds a critical value, K_{ic}, *i.e.* the fracture toughness (black line and grey plane), fracture is likely. Calculated using reference [85] with $K_{ic} = 0.32$ MPa $m^{1/2}$, as measured from Paper I.

In practice, the intended operating pressure for a given application translates into design requirements. For higher pressures, channels and other geometries must be smaller to lower the stress. The reduction in channel size must, however, be weighed against other design requirements, *e.g.* flow resistance. One example that showcases the limits is the type of inlets used for the glass chips presented in this thesis, where capillaries of circular cross-section are inserted into channels of the chip from the side, figure 5a. If channels are formed on one of two wafers by isotopic etching—meaning the aspect ratio between etch width, *w*, and depth, *d*, is equal—capillaries having an outer diameter, *D*, must fit an inlet of a minimum width $w = 2D$. If instead both wafers are processed, channels can, in theory, be circular, and $w = D$. Effects such as etch surface variations, wafer misalignment, figure 5b, and the need to have an opening in the etch mask forces however designed widths to be made larger than what is theoretically possible. Using models of bulging plates [85], the pressure tolerance can be estimated by the stress intensity factor, K_i, which describes the stress state at a crack tip. For a channel, K_i increases with pressurization and when it exceeds the fracture toughness, a fracture is likely to occur. When the

wafer thickness is considerably larger than the channel width, shearing of the material dominates and the pressure tolerance scales as $P \propto w^{-1}$, figure 5c. Thus, by utilising double-sided etching, the strength of such chips can be increased.

Integrated electrodes

Integration of metal thin film, typically, Al or Cu, in silicon is readily done in silicon-based electronics. To achieve this, thin films are usually first embedded into the silicon on a diffusion barrier and then planarized by polishing to achieve a flat and bondable surface [86].

By integrating metal thin films into the glass chips, the functionality of the chips can be greatly increased, allowing for both sensor and actuator applications. Fabrication methods put requirements on which materials that can be integrated, and therefore also limit which applications that are possible to pursuit. By integrating conductive metal, sensor elements relying on resistance (used in Paper IV and VI) or dielectric measurements (used in Paper V and VI) were made possible. By creating a direct contact to the fluids, localized heating can also be done (used in Paper IV and VI). The metal of choice in this thesis was platinum. Platinum is used for several reasons: it is a noble metal of high melting point (1768 °C) and it can thereby withstand the temperature of the thermal treatment (625 °C) performed during the fabrication to achieve strong bonding. It is further chemically inert to the strong oxidizing agent used in the processing, hot nitric acid, and has a high corrosion resistance. Advantageous for temperature sensing, the resistivity has a highly linear response to temperature [87]. For thin films of noble metals to better adhere to oxide-based substrates such as glass, thin (~20 nm) adhesion layers of either titanium or tantalum were used. Both metals form oxides in the metal-substrate interface and, at higher temperatures, tantalum has better adhesion properties than titanium [88].

Fabricating in glass

The bulk building material used in this thesis, borosilicate glass, is typically supplied in the form of 1.1 mm thick, diameter 100 mm, wafers. By its manufacturing, it is an unpolished float glass having a total thickness variation of less than ± 50 µm. In this regard, it is different from silicon wafers which typically are polished and lapped down to higher levels of flatness. To create glass chips, the following steps are typically needed: cleaning, etch mask formation, lithography, etching, bonding, thermal treatment.

1. A typical fabrication starts off with cleaning, which due to the oxidized state of the glass, can be done by both an oxygen plasma treatment and strong oxidizing acids such as nitric acid. By this treatment, a high level of organic, inorganic and metal contaminants are removed.
2. The next step is to create an etch mask from which structures can be defined. As opposed to silicon, where the native oxide of material can be used for such purposes, such mask must be added. The choice of etch mask material is first of all dependent on the etch rate selectivity between the mask and bulk material. The etchant, hydrofluoric acid, readily attacks oxides and can, if the concentration of the etchant is high or if long etch times are used, diffuses through polymeric films such as photoresist. When photoresist cannot be relied on as an etch mask, metal is typically used, *e.g.* Cr-Au [75] or Mo [75]. For the mask to be effective, cracks and pinholes in the film must be minimized, which can occur from insufficient cleaning or tensile stress being formed by the thin film deposition. For extra protection when deeper structures are etched, a thick (~12 μm) hard-baked photoresist film on top of the metal can be used. In this thesis, evaporated Cr-Au masks were used in Paper II and III and sputtered Mo masks were used in the other papers.
3. The patterning of the etch mask is done with UV lithography. For flat wafers, photoresist can be added by spinning, leaving a thin (~1.1 μm) resist film. In this thesis however, the chips had structures with different etch depths (2 in Paper I, II, III, VII, and IV; 3 in V and VI), forcing the need to add the photoresist by spray-deposition in subsequent fabrication runs. Such films give a higher thickness (~12 μm). Once the photoresist is exposed and developed, the metal masks must be etched. For Cr-Au masks, a two-step etch is done using an iodide-based etchant for Au and a ceric ammonium nitrate-based etchant for Cr. For Mo, a solution containing nitric acid, hydrochloric acid, phosphoric acid and acidic acid can be used. When processing on Mo, a photoresist adhesion promoter (hexamethyldisilazane, HDMS) is used.
4. Glass etching is done using hydrofluoric acid, which depending on the depth of the etch is performed using in either concentrated (51 wt.%) form or buffered (1:7 $HF:H_2O$ with ammonium fluoride) in a lower concentration. The concentrated solution, which has an etch rate of about 6.9 μm/min, is used for deep etching (10-200 μm) and the buffered solution, which has an etch rate of about 20-30 nm/min, is used for thin sub-μm etching for embedding electrodes. After the etch, the photoresist is stripped in acetone, isopropanol, followed by an oxygen plasma treatment. The masking metal

is removed by their respective enchant. When more etched structures of different depths are used, step 1-4 are repeated.

5. To join the processed wafers together, hydrophilic bonding is done. Wafers are first treated in an oxygen plasma and then in 69% nitric acid for 15 min at 80 °C. Then, the wafers are rinsed in water and bonded. For the removal of particles, a short acoustic cleaning treatment of with potassium hydroxide can be added before the nitric acid treatment. With the treatment, the surface of the glass becomes hydrophilic as a hydrolyzed glass layer is formed [85]. After the bonding, the wafers are thermally treated at 625 °C for 6 h. At this temperature, the glass is slightly viscous (~ $10^{10.5}$ Pa · s), which help in sealing the bond interface.

For the integration of electrodes, an extra fabrication step is added. Similar to step 2-4, ~100 nm scale trenches are first etched using a metal mask. These trenches are then filled with the electrode thin film by sputtering either Ti-Pt or Ta-Pt to a matching thickness. After lift-off, where the photoresist and metal etch mask is removed, the electrode material becomes embedded on the surface of the glass, ideally having its surface in the same plane as that of the wafer. If the electrodes are too high, bonding will be hindered. If the electrodes are to low or if too much under-etch occurs, fluid might leak through the electrode-glass interface. When the height mismatch is about 30 nm or less; bondable, leak-free and pressure tolerant chips can be made. The integrated electrodes were either processed on a single wafer having no channels etched into them (used in Paper IV), or, the electrodes were fabricated on wafers containing etched channels (used in Paper V and VI). By the later method, electrodes could be allowed to follow down along the etched sides of the channels and be used in more advanced geometries, *e.g.* parallel plate capacitors.

Backend fabrication, mounting and component integration

While chips make up for the core technology behind microfluidics, the integration of them to their surrounding is a central aspect for any application to be realized in practice. For the systems which are used in this thesis, the following interfaces must be considered:

- Fluid connections. Fluids must enter chips from both pumps and, when more than one chip is used, other chips. The high pressures put considerable requirements on the chips, but also on the fluid connections and associated tubing. In general, such fluid connections can be achieved by clamped fixtures [79], laser welding [89]

or glued capillaries. In this work, silica capillaries were glued from the side of the chips. Such capillaries can then be connected to strain-relieved standardized (*i.e.* 1/16" stainless steel) tubing.

- Optical access. To be able to study the flow behavior in chips, some form of optical access is typically required. Having optical access from both sides of the chips is ideal for imaging purposes, as it allows for absorbance measurements and high-intensity direct light which is important for high-speed imaging.
- Electrical connections. By the integration of electrical elements in chips, so follows the need to have electrical connections. This requires accessible connection pads which are compatible with the fabrication. In this work, pads are placed on the sides of the chips and access is created by three different methods: direct contact of the thin film cross-section, etching out a space between the thin film and the glass, or by combining etching and dicing to achieve a top open pad.
- Temperature control. For studies which use CO_2, fluid properties are largely affected by temperature. Therefore, precise temperature control of both the chip and the connections allow studies to be performed with both higher accuracy and over different fluid conditions. To achieve this, chips can be mounted in thermal contact with temperature controlled fixtures.

With chips having a size of roughly 1 cm^2, a lot of interfacing is needed on a small surface, as fluid connections, electrical connection, optical access and temperature control must be dealt with. Some priorities, dependent on the application, are made. In Paper I, II, III, and VI, chips were mounted on temperature controlled fixtures, but this hindered transmission lighting. Likewise, in Paper IV, V and VII, chips were mounted in a transmission light setup, which hindered precise temperature control.

In Paper VI, figure 6, complexity was further increased as four different chips were used together, where three of them use electrical circuits. This puts increased requirements on the reliability of the system. As the complexity of the system increases, the risk that whole system will fail—due to a single component-failure—increases. Therefore, in Paper VI, a printed circuit board was introduced which had robust chip-to-board electrical connections, electrical pin mounting and through-hole mounting of tubing.

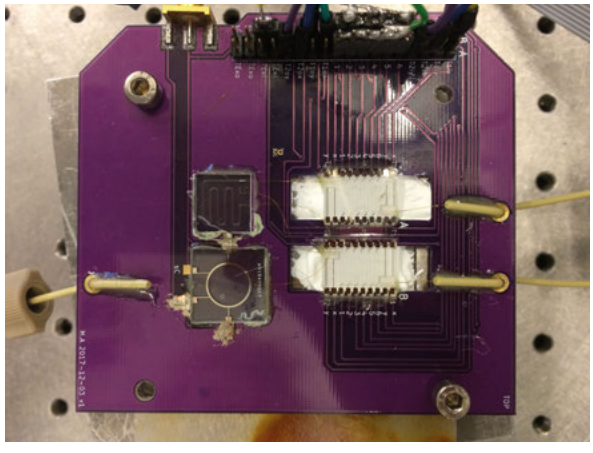

Figure 6. The flow control board used in Paper VI, showing the mounting of chips, the electrical connections and the through-hole mounting of tubing.

Sensors and actuators

Temperature sensors

In Paper IV and VI, temperature sensors were constructed. Such sensors work by measuring the resistance over a specific region of the thin film and correlating the change in resistance with temperature. Due to the high linearity between the resistivity of Pt with temperature, only a linear calibration between the measured resistance and an external reference thermometer is needed. To achieve a locational specific measurement, *e.g.* directly before and after the heater in Paper IV, resistance was measured in a 4-terminal configuration. By having the sensor element (*e.g.* section of thin film placed as a meander) connected to two conductors on each end, a supply current could be passed over the sensor element from two conductors to generate a voltage drop, which then, by the other two conductors, could be measured. Since only a very low current was passed over the two sensing conductors, their voltage drop was negligible and only variations of temperature in the sensing element were picked up by the measurement.

Flow sensors

A central component of flow control is flow sensors. There are several different working principles that can be used for this, originating from mechanical, pressure or thermal properties. In Paper IV, a thermal transfer sensor of calorimetric type was integrated into high-pressure glass chips and used to sense the flow rate, figure 7. A calorimetric flow sensor consists of a pair of temperature sensors with a heater in between [86]. During zero flow, when the heater was turned on, a uniform thermal boundary layer forms around the heater. As flow is applied, the temperature distribution of this layer changed and becomes asymmetrical. By placing one temperature sensor upstream and the other downstream, this change can be measured. For common gases and liquids where properties only vary slightly with temperature, an approximatively linear range can often be used. As the thermal boundary layer can be affected by other means than the velocity, *e.g.* by the Prandtl number, flow measurements of CO_2 in the supercritical regime by this method are more challenging. In Paper IV, it was shown that flow sensing of dense CO_2 microflows was possible with the sensor both at a liquid and a supercritical state. However, when

conditions are close to the critical point, properties vary a lot, and the flow response does too.

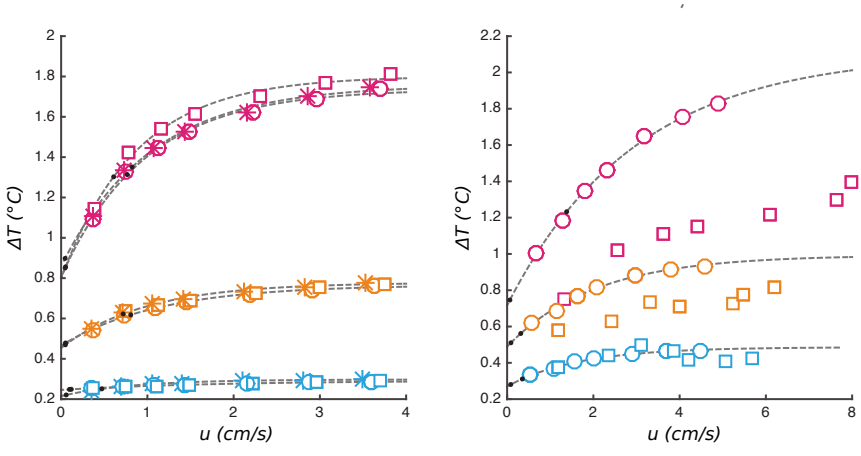

Figure 7. Flow sensor response of CO_2 at either liquid (left) or supercritical (right) conditions. The measured temperature difference, ΔT is shown as a function of velocity, *u* with the heater driven at 1 (blue), 3 (orange) or 5 mA (violet). (left) For liquid conditions at 18-23 °C and 80 (square), 100 (circle) and 120 (star) bar, the response shows a predicable behaviour. (right) For supercritical conditions at 33–46 °C and 100 bar, the flow response was also predictable. Close to the critical point, at 80 bar, the flow response became unsteady. Data from Paper IV.

Relative permittivity sensors

By measuring the relative permittivity of fluids, key properties of the fluids can be measured and studied. In a direct sense, it offers a measurement of the polarity of fluids as the relative permittivity is strongly affected by the dipole moment, d_μ , by (1). The relative permittivity is also affected by changes in density (*i.e.* the molar volume, V_f). This is highly useful for studying compressible fluids that have varying density, which otherwise often must be approximated from measurements of pressure and temperature. For the interesting multicomponent fluids that combine CO_2 and polar solvents, used in chromatography and various high-pressure applications, another parameter can be sought for—composition. By a descriptive model, such as the one in (2), a relationship exists between the relative permittivity and the composition of the mixture. If the properties of the pure components and this relationship are known, for binary component fluids, the composition can be measured.

There are several ways to measure dielectric properties. Methods include: coaxial probes, waveguides, resonant cavities and parallel plates [90]. In Paper

V, a parallel plate sensor was introduced, having a high pressure tolerant fluid channel in between the plates. By using a parallel plate geometry with no other material between the electrodes other than the fluid, the interpretation of measurement became straightforward and related as follows,

$$\varepsilon_r = \frac{C}{\varepsilon_0}\frac{d}{A} \quad (10)$$

where ε_0 is the permittivity of vacuum, C is the capacitance and d/A is the ratio between plate height and area. ε_r is a frequency dependent number, but at frequencies less than about 10 MHz, it deviates only slightly from the static relative permittivity (*i.e.* at zero frequency) and can be determined at frequencies where electrochemical effects between the fluids and the electrodes will not interfere with measurements [91,92]. The capacitance can then be determined by measuring the impedance, *e.g.* by using a vector network analyzer.

Heat actuators

Integrated electrodes can not only be used for sensing applications, but also for actuation. In Paper VI, a chip was introduced that had a flow restricting channel with an integrated heating element. By cooling the chips and having the integrated heaters in direct contact with the fluid, an exact and fast method of changing the fluid temperature was provided. This affected the viscosity and density, leading to an actuation on the flow rate. While this method of actuation is highly linked to the type of fluid which passes the restrictor, it offers a way to fine tune flow rates without mechanical components. Similar to a throttling valve, small changes of the applied heat output lead to small and predictable changes in flow. Just as for the flow sensor in Paper IV, the behaviour was complex when heat was applied to a CO_2 flow in regions around its critical point. Effects include the changing Prandtl number and local minimum formed by the viscosity and density ratio.

Implementation

Data collection

As has been demonstrated in this overview, handling microflows of high-pressure fluids require an extensive need for understanding, sensing, and control. With the possibility arising from combining sensor elements and actuators with automated and computer-based data logging, control system, and model-based calculations—handling and understanding of high-pressure microflows have become increasingly more available. All papers in this thesis used sensing, either internally in chips or externally from the supporting fluid equipment, to form a combined picture of the fluid at flow by measurement of properties, *e.g.* pressures, temperatures, and flow rates. By turning to flow-based continuous studies—instead of the traditional method of working with batched-based experiments—the rate of data collection and parameter space, which can be easily accessed in short timescales, can be increased. While only Paper II and IV actually surveyed different pressure and temperature conditions, Paper V, VI, and VII demonstrated chip based measurement systems which all hold promise for fast data acquisition. For high-throughput data collection in extraction studies, chips similar to those in Paper III could be used.

Image processing and analysis

In Paper, VII, where a system was presented which could measure the effect that additive salts have on pH in a CO_2-water environment, data collection was extended further as data from images were collected, processed and analysed in an automated manner, figure 8. The planar form-factor is an advantage for microfluidics, and maybe as opposed to capillary fluidics, it couples well with image analysis. The optical view field over the entire chip was held fixed and by combining code and chip design, large sets of data could be acquired from a single image. Explored in Paper VII, high-speed imaging, which is necessary to capture many dynamic effects in microflows, typically gives highly redundant data, but by automatically processing this information, the time and spatially resolved data was extracted easily.

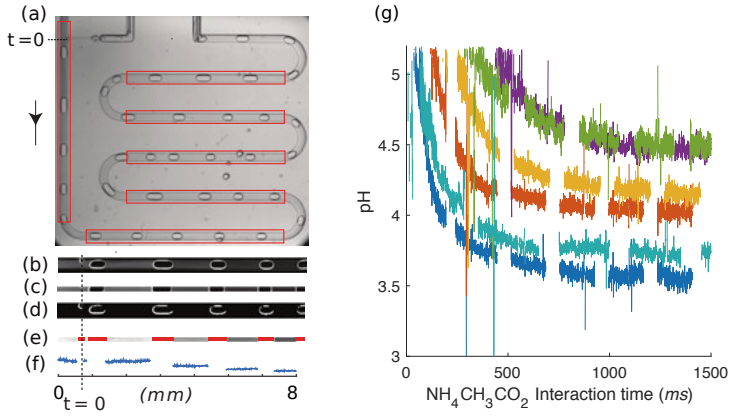

Figure 8. Automated image processing pipeline of high-speed imaging data. Video was recorded at 1200 frames/s and for each frame, the pipeline was used to extract the light absorbance of aqueous solutions in contact with CO_2. The two fluids formed segments which flowed along a meander. From the image (a), reference points were defined from known features which were then used to determine 6 processing regions (red rectangles). Aligned by the reference points, the image was then compared to another blank image and absorbance was calculated pixel-wise, allowing for 6 absorbance images of the channel defined by the processing regions (b). Following centring and removal of channel edge data, 6 measurement regions (c) were defined. With a binary image tuned to detect edges (d), the CO_2 segments could be filtered (red regions) and the final measurement regions (e) was defined. By this, absorbance of the aqueous phase as a function of channel length could be determined. The location of the contact point when CO_2 and water first meet is indicated by t = 0. By sampling for 0.25 s, an averaged absorbance image over the channel can be formed, and with calibration to a pH sensitive dye, used to measure the change in pH as a function of time (g) for solutions containing different concentrations of ammonium acetate.

Control systems

When both sensor and actuators can be combined in a shared microfluidics system, control of properties becomes possible. This was demonstrated in Paper VI, where a relative permittivity sensor and two heat actuators were used in a closed control system to regulate a high-pressure microflow of CO_2 and methanol. One example of this is shown in figure 9. By determining the relative permittivity of the flowing mixture, the value can be compared to a reference and, depending on the difference, the flow resistance in the heated actuators can be changed. If the fluid mixture is well characterized, the relative permittivity can then be used to determine the composition of the mixture. By extension, this then allows for precise control and tuning of the composition of the mixtures.

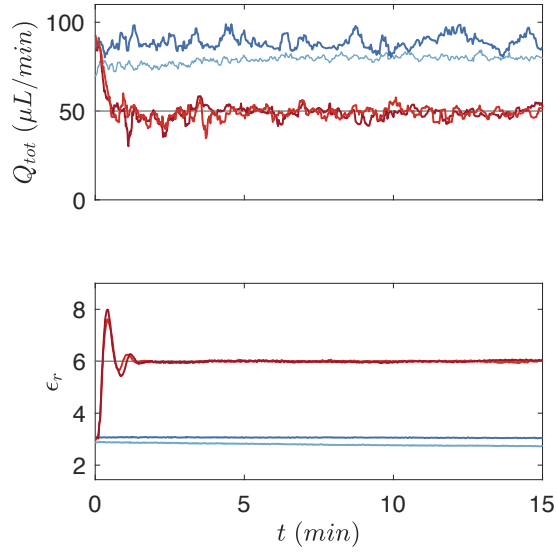

Figure 9. Use of the control system in Paper VI, when used to control both the total flow rate Q_{tot} (top) and the relative permittivity, ε_r, (bottom) of a CO_2-methanol mixture driven from a shared constant pressure source. Two replicated runs are shown with the system turned on (red) and turned off (blue). When the system was turned off, the total flow rate was 85 µL/min and the relative permittivity was 2.9. By activating the control system, Q_{tot} and ε_r were changed and reached there an asked for value, *e.g.* set points (grey line).

Concluding remarks - Combining it all together

Combining modular systems

By combining different chips and turning to a multi-chip design, as in Paper V and VI, modular systems of higher complexity can be created, giving a larger freedom of design for both applications and in fabrication. As opposed to designing all functionality on a single chip, there are several advantages of the multi-chip approach: by a few different chips, a larger range of functions can be realized and changed depending on the application; fabrication becomes independent between the components, which offers both more design choices and an increased yield of production; standardization of components becomes possible which allows for evading redesign of common functional elements (*e.g.* mixing chips).

The variable properties of CO_2 can make microflows challenging to handle, but, by introducing new components, added control is possible. A striking example of this was the measurements of the relative permittivity of CO_2 with either ethanol or methanol, done in Paper V and VI, respectively. For the measurements in Paper V, different flow conditions were achieved by changing pump pressures. By that method, large variations in perceived pump flow rate were seen as the whole CO_2 volume comprised in a pump must change to new equilibrated conditions. By that method, a flow model was needed to describe the flow at the relative permittivity sensor. For the measurements in Paper VI, the situation was very different. Here, changes in flow were achieved by the flow regulating actuator chips, and the CO_2 volume of the pump and tubing sensor could be kept compressed and at an equilibrated state. Consequently, variations in flow for those measurements are low, and new flow conditions could stabilize in less than half a minute. Thus, by combining microfluidic actuators and sensors; data collection and mapping can be done more efficiently.

By combining the sensor with actuators, either the pumps or heating chips, control systems can be realized. This extends the benefit of microfluidic sensing elements to not only measure variable properties but also keeping them

stable and constant—a concept of high importance in miniaturized chemical analysis.

Future outlook

With modular systems, the systems presented in this thesis could be easily expanded. For example, by combing the composition and flow control system of Paper VI with the chips used in Paper III and VIII, some very interesting studies could be made possible. It would then be possible to conduct studies on either flow behavior or pH with precisely defined multicomponent fluids at high pressure. With the flow-based and automated data processing methods shown in Paper VII, the collection of data over a wide parameter space should become possible. Furthermore, with these control components, new routes can be taken into creating miniaturized—widely available—platforms for chemical analysis at high pressure.

Meanwhile, the pressure tolerance of glass chips still has a lot left to ask for. As the solvent power of pure CO_2 is still relatively weak for many interesting chemical compounds at the pressures from where the chips used in this study were operated at high reliability, increased pressure tolerance of microfluidic chips is highly sought out for. By introduction of other materials or fabrication methods, this should, however, become possible in the future.

Sammanfattning på svenska

Dagens samhälle drivs allt mer av att det finns information för att kunna ta bra beslut. En del av detta informationsbehov avser kemiska frågeställningar. Till exempel behöver en läkare veta hur länge ett läkemedel verkar, markägare och myndigheter behöver veta om deras mark är förorenad och en tillverkare av livsmedel behöver säkerställa att tvättprocesser inte lämnar kvar rester. För att få fram informationen behövs verktyg.

Verktyg som kan mäta olika kemiska parametrar, t ex mängden av en viss kemisk förening, är ofta komplexa och behöver innehålla många olika komponenter som samverkar för att åstadkomma en given funktion. Därmed blir verktygen i många fall dyra, stora och bundna till en fysisk lokal, t ex ett laboratorium. Det gör i sin tur att den kemiska mätningen blir otillgänglig. Tester blir också dyra och svåra att åstadkomma på udda platser och tillfällen.

För att öka tillgängligheten av kemiska mätningar finns ett intressant koncept som denna avhandling behandlar: miniatyrisering. Genom att göra saker mindre fås flera fördelar. Bland annat kan fler funktioner rymmas på en mindre yta och det går åt mindre mängder material för att åstadkomma uppgiften och fenomen som enbart uppstår vid små längdsskalor kan användas. På så vis kan miniatyrisering skapa kemiska mätverktyg som blir mindre och effektivare.

En intressant grupp av kemiska mätverktyg använder flöden av vätskor för att åstadkomma mätningar och för att de ska kunna genomföra mätningar snabbt och med stor noggrannhet behöver vätskeflödet hålla ett högt tryck och flöda på ett kontrollerat sätt. Genom att också värma och trycksätta en gas eller vätska till en så kallad superkritisk fluid, som löst kan beskrivas som ett mellanting av en vätska och en gas, kan speciella egenskaper erhållas och användas för att göra kemiska mätverktyg ännu bättre. En gas som ofta används är koldioxid.

Om man pressar ihop gas av koldioxid till en liten volym blir gasen tillslut till en vätska. Fortsätter man att trycksätta till ungefär 74 gånger trycket av vanligt atmosfärstryck och samtidigt värmer till mer än 31°C, blir koldioxid superkritisk. Koldioxiden blir då så tät att den går att använda som ett lösningsmedel.

Samtidigt är den väldigt rinnig (låg viskositet och liten friktion), vilket gör att kan får att flöda genom små kanaler.

Förmågan hos fluider att flyta med låg friktion är en egenskap som är väldigt intressant för miniatyrisering då kanaler där ofta är små. Koldioxiden har då, likt gas, ett kompressibelt beteende, där egenskaper så som täthet och rinnighet förändras med olika tryck och temperaturer. Koldioxiden blir därmed också svår att hantera. T ex påverkas tätheten om trycket förändras, vilket gör att det inte nödvändigtvis behövs lika stor volym koldioxid in i en kanal som ut ur en. Det ställs därför höga krav på mätverktyg som använder superkritisk koldioxid.

Komponenter i verktygen, t ex flödesmätare och ventiler, måste tåla höga tryck och få vätskeflödena att bete sig på ett kontrollerat sätt. Ska sådana komponenter sedan miniatyriseras gäller samma, eller högre, krav. I denna avhandling presenteras sådana miniatyriserade flödeskomponenter—gjorda för att på olika sätt hantera flöden av koldioxid.

Genom miniatyrisering kan funktioner, så som flödeskanaler, sensorer och ventiler, byggas in i små enheter, så kallade chip. För att kunna göra det och samtidigt hantera flöden under högt tryck behövs förståelse för vad som påverkar trycktåligheten och fluiders flödesbeteende. Detta behandlas i denna avhandling. Genom att följa trycktålighet i olika kemiska miljöer över tid har det kunnat visas att chip gjorda av glas påverkas inte bara av det pålagda trycket utan också utav belastningstid och miljö.

Ett flödesfenomen som studeras i detta arbete är att superkritisk koldioxid och vatten kan fås att flöda längs med varandra på ett kontrollerat sätt. Detta tros i framtiden kan komma att nyttjas för att förbereda prover för kemiska mätningar. När längdskalor blir små beter sig flöden på andra sätt. T ex kan krafterna som uppstår av ytspänning bli högre än tyngdkraften. Likt olja och vatten, är koldioxid och vatten inte blandbara, vilket gör att de typisk flödar i uppdelade segment. Genom att förändra både vätningsegenskaperna (så ytan blir mera vattenavvisande och koldioxid mera vätande) och formen på en flödeskanal, kan möjligheterna för att fluiderna ska flöda bredvid varandra, istället för i segment, ökas.

För att kunna hantera små flöden i chip behövs också system som kan ställa och reglera flödesbeteendet. Det är t ex önskvärt att ett flöde har en noggrant känd flödeshastighet eller en bestämd kemisk sammansättning. Detta behandlas också i detta arbete där flera givare, så som flödesensorer, temperatursensorer och permittivitetssensorer, har utvecklats för små flöden under högt tryck. Permittivitet beskriver påverkan mellan ett elektriskt fält och ett elektriskt isolerande material, och bestäms av materialets förmåga att förskjuta sina

laddningar. För att kunna bygga sådana system har en tillverkningsmetod använts som tillåter att elektriska ledare kan integreras på olika sätt i högtryckståliga chip. Detta har givit möjligheten att kunna mäta temperatur lokalt i flödeskanaler och på så sätt har man kunnat se att temperaturvariationer kan uppstå i samband med tryckfall hos små flöden av koldioxid. Vidare har det kunnat visats att flödesensorer för superkritisk koldioxid också kan integreras i chip, vilket därmed möjliggör för att flödeshastigheter kan mätas lokalt i trycksatta chip.

För flertalet kemiska verktyg som använder koldioxid räcker det dock inte att bara använda ren koldioxid, utan ofta behöver det också tillsättas andra lösningsmedel, t ex alkoholer. Förutsatt att trycken är höga kan koldioxid och alkoholer lösa sig i varandra och därmed bete sig som en sammansatt vätska. Det blir då också viktigt att noggrant kunna ställa in förhållandet mellan mängden koldioxid och mängden alkohol som flödar. Beteendet av sådana sammansatta vätskor ändrar sig betydligt beroende på förhållandet av koldioxid och alkohol. I denna avhandling har det därför utvecklats en sensor som kan känna av sammansättningen hos små flöden under höga tryck.

Sensorn kan mäta den så kallade relativa permittiviteten hos fluider, en egenskap som beskriver hur svårt ett material har för att inrätta sig i ett elektriskt fält. Typiskt skiljer sig den relativa permittiviteten åt för olika lösningsmedel, den är t ex typiskt låg för oljor och koldioxid och hög för alkoholer och vatten. Denna skillnad, som med sensorns hjälp går att mäta, kan sedan användas för att ta reda på sammansättningen hos små flöden bestående av t ex koldioxid och alkohol. Vidare möjliggör sensorn också för att kunna studera den relativa permittiviteten hos andra fluider vid höga tryck.

Även om det går att noggrant karakterisera flöden med hjälp av enbart sensorer så behövs det ytterligare en funktionalitet för att kunna nyttja flöden av koldioxid och alkohol: ställbarhet. I avhandlingens arbete har det därför också skapats ett chip som kan ändra på flödesmotstånd—likt en ventil eller ett ställdon. Förändringen i flöde sker genom att via värme ändra fluidernas täthet och rinnighet. För att skapa ett flöde bestående av sammansatt koldioxid och alkohol kan flöden av ren koldioxid och alkohol mötas i en punkt där de mixas samman. Genom att sedan placera två sådana flödesförändringschip innan mixningspunkten kan förhållandet mellan koldioxid och alkohol ändras och därmed ställas in till ett önskat läge. Den sammansatta vätskan får både en förändrad sammansättning och en förändrad relativ permittivitet som kan mätas. Flödesförändringschipen och sensorn kan samverka i ett återkopplat system där flödesmotståndet ändras tills att sensorn uppfattar ett visst värde av relativ permittiviteten som man på förhand har önskat ställa in.

Att studera relativt vanliga, men viktiga, egenskaper hos vätskor, t ex hur sur en lösning blir, kan vara svårt för fluider som både behöver vara trycksatta och kan ändra sitt beteende vid olika tryck och temperatur. Till exempel gör de höga trycken att fluiderna behöver vara inneslutna i stängda behållare. Då dessa fluider typiskt används i flödande system där tryck och temperatur kan variera över tid och rum blir det svårt att veta vad som händer med dem. Det behövs därför också verktyg för att mäta och förstå sådana förlopp. I denna avhandling presenteras ett sådant instrument. Där studeras den försurning som sker när koldioxid och vatten blandas i hög upplösning i såväl tid och rum.

Acknowledgement

First of all, I would like to thank *Klas* and *Roger* for letting me have the opportunity to start this research and develop myself. It has been a nice journey. *Klas,* you valuable advises and guidance throughout the years have been most appreciated.

For my supervisor, *Lena*, who has guided me through this adventure, I am ever so grateful. Your hard work, in both the lab and in writing, has shown me the way forward and helped me in realising many ideas. It has been a pleasure creating this thesis with your support. Also, by the courses you have led, many students, including me, have found the liking of the miniaturized world.

Charlotta and *Irene* at Lund University, your insight into the chemistry and applications of CO_2 have been central to this work and my development here over the years. At KTH, I want to thank *Gustav A* for your input on the fluid dynamics.

This work would not have been possible without the help from the Microstructure Laboratory (MSL). Over the years, I have etched at least a cm of glass and deposited close to a tenth of an mm metal in your lab. Thank you, *Leif*, *Björn*, *Amit*, *Rimantas*, *Farhad* and *Örjan* for both teaching me how to operate the process equipment as well as making sure that it is in shape. Thank you, *Fredric*, *Jan-Åke* and *Victoria* for giving me the eyes to see what I do. The help in using SEM and VSI has been most appreciated. I also would like to thank the cleaners of MSL, you too, are central for making chips.

I have learned a lot from my colleagues, in fields I never thought before I would use, and therefore, I owe them a very special thank you:

Stefan K for first showing me around the lab and teaching its workings.
Atena and *Martin B*, for telling me what RF and electronics can do.
Sam, *Klas*, *Roger*, *Lena* and *Stefan K*, for introducing me to high pressures.
Pontus and *Javier*, for telling me about wetting, pinning and cool surfaces.
Ernesto, for showing me how you push the borders of a dry etcher.
Hugo, for teaching me how to draw my first line in CAD.
Fredric, for our hunt of NiSn and AgIn.
Anders, for introducing me to microplasmas.

Mats, for the discussions about optics, control and university.
Maria T and *Mathias*, for introducing me to cells and acoustics.
Zhigang, for teaching me about microfluidics.

While less related to research, I also would like to thank *Frida, Simon, Karolina, Ana-Maria, Sean, Sarah, Federico* and all the other colleagues of MST for keeping the office a happy place. *Peter,* thank you for telling me about all the cool stuff you do in Försvarsmakten. *Stefan J,* thank you for the nice lunch discussions. *Ming-Zhi, Alireza*, *Shung-Hee* and all the people of EMBLA, I have very much enjoyed hanging out with you at the office and hear about your exciting projects. I would also like to thank *Jesper*, *Krishna*, *Anton* and *Simon* for letting me supervise your master theses—together we have explored many exciting ideas of high-pressure systems and microfabrication. Thank you, *Per-Richard*, *Sara,* and *Maria M* for helping me buy peculiar things from peculiar places, and thank you *Jonatan* for trying to install them. For the people in the MiM and Tribo groups, I have really enjoyed your company. Furthermore, I really appreciated the help I got from *Henrik*, *Sofia,* and *Björn*, who showed me how patents work. Furthermore, *Johan E* and *Niklas R,* thank you for being a helpful hand in discussions about various chemical endeavours.

Finally, *Jiao,* no support is greater than the one you have given me.

References

[1] T.W. Murphy, Q. Zhang, L.B. Naler, S. Ma, C. Lu, Recent advances in the use of microfluidic technologies for single cell analysis, Analyst. 143 (2018) 60–80. doi:10.1039/C7AN01346A.

[2] A.M. Streets, Y. Huang, Chip in a lab: Microfluidics for next generation life science research, Biomicrofluidics. 7 (2013) 11302. doi:10.1063/1.4789751.

[3] J.S. Mellors, W.A. Black, A.G. Chambers, J.A. Starkey, N.A. Lacher, J.M. Ramsey, Hybrid Capillary/Microfluidic System for Comprehensive Online Liquid Chromatography-Capillary Electrophoresis-Electrospray Ionization-Mass Spectrometry, Anal. Chem. 85 (2013) 4100–4106. doi:10.1021/ac400205a.

[4] J.P.C. Vissers, H.A. Claessens, C.A. Cramers, Microcolumn liquid chromotography: Instrumentation, detection and applications, J. Chromatogr. A. 779 (1997) 1–28. doi:10.1016/S0021-9673(97)00422-6.

[5] R.E. Majors, Historical Developments in HPLC and UHPLC Column Technology: The Past 25 Years, LCGC North Am. 33 (2015) 818–840. http://www.chromatographyonline.com/historical-developments-hplc-and-uhplc-column-technology-past-25-years (accessed May 27, 2018).

[6] A. Plasz, Handbook of Pharmaceutical Analysis by HPLC, Elsevier Academic Press, 2005. doi:10.1016/S0149-6395(05)80060-1.

[7] W. Span, R; Wagner, A new EOS for CO2 covering the fluid region from the triple point temperature to 1100K at pressures up to 800MPa.pdf, J. Phys. Chem. Ref. Data. 25 (1996) 1509–1596. doi:10.1063/1.555991.

[8] O.C. Jeong, S. Konishi, Pneumatic gas regulator with cascaded PDMS seal valves, Sensors Actuators, A Phys. 143 (2008) 84–89. doi:10.1016/j.sna.2007.07.028.

[9] J. Casals-Terré, M. Duch, J.A. Plaza, J. Esteve, R. Pérez-Castillejos, E. Vallés, E. Gómez, Design and characterization of a magnetic digital flow regulator, Sensors Actuators, A Phys. 162 (2010) 107–115. doi:10.1016/j.sna.2010.04.025.

[10] A.W. Browne, K.E. Hitchcock, C.H. Ahn, A PDMS pinch-valve module embedded in rigid polymer lab chips for on-chip flow regulation, J. Micromechanics Microengineering. 19 (2009). doi:10.1088/0960-1317/19/11/115012.

[11] S. Wang, T. Wang, P. Ge, P. Xue, S. Ye, H. Chen, Z. Li, J. Zhang, B. Yang, Controlling flow behavior of water in microfluidics with a

chemically patterned anisotropic wetting surface, Langmuir. 31 (2015) 4032–4039. doi:10.1021/acs.langmuir.5b00328.
[12] K. Morita, T. Hagiwara, N. Hirayama, H. Imura, Extraction of Cu(II) with Dioctyldithiocarbamate and a Kinetic Study of the Extraction Using a Two-Phase Microflow System, Solvent Extr. Res. Dev. Japan. 17 (2010) 209–214. doi:10.15261/serdj.17.209.
[13] K. Wang, G. Luo, Microflow extraction: A review of recent development, Chem. Eng. Sci. 169 (2017) 18–33. doi:10.1016/j.ces.2016.10.025.
[14] N. Assmann, S. Kaiser, P. Rudolf Von Rohr, Supercritical extraction of vanillin in a microfluidic device, J. Supercrit. Fluids. 67 (2012) 149–154. doi:10.1016/j.supflu.2012.03.015.
[15] A. Zotou, An overview of recent advances in HPLC instrumentation, Cent. Eur. J. Chem. 10 (2012) 554–569. doi:10.2478/s11532-011-0161-0.
[16] P.G. Jessop, B. Subramaniam, Gas-expanded liquids, Chem. Rev. 107 (2007) 2666–2694. doi:10.1021/cr040199o.
[17] M. Budt, D. Wolf, R. Span, J. Yan, A review on compressed air energy storage: Basic principles, past milestones and recent developments, Appl. Energy. 170 (2016) 250–268. doi:10.1016/J.APENERGY.2016.02.108.
[18] H. Yin, K. Killeen, The fundamental aspects and applications of Agilent HPLC-Chip, J. Sep. Sci. 30 (2007) 1427–1434. doi:10.1002/jssc.200600454.
[19] D.S. Reichmuth, T.J. Shepodd, B.J. Kirby, Microchip HPLC of peptides and proteins, Anal. Chem. 77 (2005) 2997–3000. doi:10.1021/ac048358r.
[20] D. Geissler, J.J. Heiland, C. Lotter, D. Belder, Microchip HPLC separations monitored simultaneously by coherent anti-Stokes Raman scattering and fluorescence detection, Microchim. Acta. 184 (2017) 315–321. doi:10.1007/s00604-016-2012-3.
[21] R.F. Gerhardt, A.J. Peretzki, S.K. Piendl, D. Belder, Seamless Combination of High-Pressure Chip-HPLC and Droplet Microfluidics on an Integrated Microfluidic Glass Chip, Anal. Chem. 89 (2017) 13030–13037. doi:10.1021/acs.analchem.7b04331.
[22] J.J. Heiland, C. Lotter, V. Stein, L. Mauritz, D. Belder, Temperature Gradient Elution and Superheated Eluents in Chip-HPLC, Anal. Chem. 89 (2017) 3266–3271. doi:10.1021/acs.analchem.7b00142.
[23] A. Ohashi, M. Sugaya, H.-B. Kim, Development of a Microfluidic Device for Measurement of Distribution Behavior between Supercritical Carbon Dioxide and Water, Anal. Sci. 27 (2011) 567. doi:10.2116/analsci.27.567.
[24] N. Assmann, H. Werhan, A. Ładosz, P. Rudolf von Rohr, Supercritical extraction of lignin oxidation products in a microfluidic device, Chem. Eng. Sci. 99 (2013) 177–183. doi:10.1016/j.ces.2013.05.032.
[25] T. Gendrineau, S. Marre, M. Vaultier, M. Pucheault, C. Aymonier,

Microfluidic synthesis of palladium nanocrystals assisted by supercritical CO 2: Tailored surface properties for applications in boron chemistry, Angew. Chemie - Int. Ed. 51 (2012) 8525–8528. doi:10.1002/anie.201203083.
[26] S. Marre, J. Park, J. Rempel, J. Guan, M.G. Bawendi, K.F. Jensen, Supercritical continuous-microflow synthesis of narrow size distribution quantum dots, Adv. Mater. 20 (2008) 4830–4834. doi:10.1002/adma.200801579.
[27] R.S. Middleton, J.W. Carey, R.P. Currier, J.D. Hyman, Q. Kang, S. Karra, J. Jiménez-Martínez, M.L. Porter, H.S. Viswanathan, Shale gas and non-aqueous fracturing fluids: Opportunities and challenges for supercritical CO2, Appl. Energy. 147 (2015) 500–509. doi:10.1016/j.apenergy.2015.03.023.
[28] B. Bao, J. Riordon, F. Mostowfi, D. Sinton, Microfluidic and nanofluidic phase behavior characterization for industrial CO2, oil and gas, Lab Chip. 17 (2017) 2740–2759. doi:10.1039/C7LC00301C.
[29] B. Bao, J. Riordon, Y. Xu, H. Li, D. Sinton, Direct Measurement of the Fluid Phase Diagram, Anal. Chem. 88 (2016) 6986–6989. doi:10.1021/acs.analchem.6b01725.
[30] B. Pinho, S. Girardon, F. Bazer-Bachi, G. Bergeot, S. Marre, C. Aymonier, A microfluidic approach for investigating multicomponent system thermodynamics at high pressures and temperatures, Lab Chip. 14 (2014) 3843. doi:10.1039/C4LC00505H.
[31] W. Song, H. Fadaei, D. Sinton, Determination of dew point conditions for CO2 with impurities using microfluidics, Environ. Sci. Technol. 48 (2014) 3567–3574. doi:10.1021/es404618y.
[32] N. Liu, C. Aymonier, C. Lecoutre, Y. Garrabos, S. Marre, Microfluidic approach for studying CO 2 solubility in water and brine using confocal Raman spectroscopy, Chem. Phys. Lett. 551 (2012) 139–143. doi:10.1016/j.cplett.2012.09.007.
[33] M. Abolhasani, M. Singh, E. Kumacheva, A. Günther, Automated microfluidic platform for studies of carbon dioxide dissolution and solubility in physical solvents, Lab Chip. 12 (2012) 1611. doi:10.1039/c2lc21043f.
[34] S.G.R. Lefortier, P.J. Hamersma, A. Bardow, M.T. Kreutzer, Rapid microfluidic screening of CO2 solubility and diffusion in pure and mixed solvents, Lab Chip. 12 (2012) 3387. doi:10.1039/c2lc40260b.
[35] S.K. Luther, S. Stehle, K. Weihs, S. Will, A. Braeuer, Determination of Vapor-Liquid Equilibrium Data in Microfluidic Segmented Flows at Elevated Pressures Using Raman Spectroscopy, Anal. Chem. 87 (2015) 8165–8172. doi:10.1021/acs.analchem.5b00699.
[36] C.E.D. Nazario, M.R. Silva, M.S. Franco, F.M. Lanças, Evolution in miniaturized column liquid chromatography instrumentation and applications: An overview, J. Chromatogr. A. 1421 (2015) 18–37. doi:10.1016/j.chroma.2015.08.051.
[37] A. Zotou, An overview of recent advances in HPLC instrumentation, Cent. Eur. J. Chem. 10 (2012) 554–569. doi:10.2478/s11532-011-

0161-0.
[38] J.P.C. Vissers, H.A. Claessens, C.A. Cramers, Microcolumn liquid chromatography: instrumentation, detection and applications, J. Chromatogr. A. 779 (1997) 1–28. doi:10.1016/S0021-9673(97)00422-6.
[39] C.E.D. Nazario, M.R. Silva, M.S. Franco, F.M. Lan??as, Evolution in miniaturized column liquid chromatography instrumentation and applications: An overview, J. Chromatogr. A. 1421 (2015) 18–37. doi:10.1016/j.chroma.2015.08.051.
[40] M. Saito, History of supercritical fluid chromatography: Instrumental development, J. Biosci. Bioeng. 115 (2013) 590–599. doi:10.1016/j.jbiosc.2012.12.008.
[41] M.A.C. Terry A. Berger, Kimber D. Fogelman, Edwin E. Wikfors, L. Thomson Staats, III, Samuel O. Colgate, Compressible fluid pumping system for dynamically compensating compressible fluids over large pressure ranges, US 8215922B2, n.d.
[42] M. Saito, Y. Yamauchi, H. Kashiwazaki, M. Sugawara, New pressure regulating system for constant mass flow supercritical-fluid chromatography and physico-chemical analysis of mass-flow reduction in pressure programming by analogous circuit model, Chromatographia. 25 (1988) 801–805. doi:10.1007/BF02262088.
[43] M.C. Terry A. Berger, Samuel Colgate, US8419936B2: Low noise back pressure regulator for supercritical fluid chromatography, 2013.
[44] W.M.H. J. F. Ely, J.W. Magee, Thermophysical Properties for Special High CO2 Content Mixtures, GPA Res. Rep. (1987) 1–161.
[45] P. Raveendran, Y. Ikushima, S.L. Wallen, Polar attributes of supercritical carbon dioxide, Acc. Chem. Res. 38 (2005) 478–485. doi:10.1021/ar040082m.
[46] A. Fenghour, W.A. Wakeham, V. Vesovic, The Viscosity of Carbon Dioxide, J. Phys. Chem. Ref. Data. 27 (1998) 31–44. doi:10.1063/1.556013.
[47] A. Tabernero, E.M.M. del Valle, M.Á. Galán, A comparison between semiempirical equations to predict the solubility of pharmaceutical compounds in supercritical carbon dioxide, J. Supercrit. Fluids. 52 (2010) 161–174. doi:10.1016/j.supflu.2010.01.009.
[48] M. McHugh, V. Krukonis, Supercritical fluid extraction: principles and practice, (2013) 512. https://books.google.es/books?hl=es&lr=&id=VTIvBQAAQBAJ&oi=fnd&pg=PP1&dq=McHugh+%26+Krukonis,+2013+co2&ots=QHacQUWRvP&sig=On4-TQvxT1rJPT2c2C-2yeIvGtQ (accessed May 28, 2018).
[49] C.J. Chang, C.-Y. Day, C.-M. Ko, K.-L. Chiu, Densities and P-x-y diagrams for carbon dioxide dissolution in methanol, ethanol, and acetone mixtures, Fluid Phase Equilib. 131 (1997) 243–258. doi:10.1016/S0378-3812(96)03208-6.
[50] K. Bezanehtak, G.B. Combes, F. Dehghani, N.R. Foster, D.L. Omasko, Vapor-liquid equilibrium for binary systems of carbon

dioxide + methanol, hydrogen + methanol, and hydrogen + carbon dioxide at high pressures, J. Chem. Eng. Data. 47 (2002) 161–168. doi:10.1021/je010122m.
[51] A.P. Abbott, E.G. Hope, R. Mistry, A.M. Stuart, Probing the structure of gas expanded liquids using relative permittivity, density and polarity measurements, Green Chem. 11 (2009) 1530. doi:10.1039/b915570h.
[52] R. Sih, F. Dehghani, N.R. Foster, Viscosity measurements on gas expanded liquid systems-Methanol and carbon dioxide, J. Supercrit. Fluids. 41 (2007) 148–157. doi:10.1016/j.supflu.2006.09.002.
[53] C. West, J. Melin, H. Ansouri, M. Mengue Metogo, Unravelling the effects of mobile phase additives in supercritical fluid chromatography. Part I: Polarity and acidity of the mobile phase, J. Chromatogr. A. 1492 (2017) 136–143. doi:10.1016/j.chroma.2017.02.066.
[54] A. Grand-Guillaume Perrenoud, J. Boccard, J.L. Veuthey, D. Guillarme, Analysis of basic compounds by supercritical fluid chromatography: Attempts to improve peak shape and maintain mass spectrometry compatibility, J. Chromatogr. A. 1262 (2012) 205–213. doi:10.1016/j.chroma.2012.08.091.
[55] Y. Cui, S. V. Olesik, Reversed-phase high-performance liquid chromatography using enhanced-fluidity mobile phases, J. Chromatogr. A. 691 (1995) 151–162. doi:10.1016/0021-9673(94)00878-D.
[56] S. Al-Hamimi, A. Abellan Mayoral, L.P. Cunico, C. Turner, Carbon Dioxide Expanded Ethanol Extraction: Solubility and Extraction Kinetics of α-Pinene and cis-Verbenol, Anal. Chem. 88 (2016) 4336–4345. doi:10.1021/acs.analchem.5b04534.
[57] T. Teutenberg, S. Wiese, P. Wagner, J. Gmehling, High-temperature liquid chromatography. Part III: Determination of the static permittivities of pure solvents and binary solvent mixtures-Implications for liquid chromatographic separations, J. Chromatogr. A. 1216 (2009) 8480–8487. doi:10.1016/j.chroma.2009.09.076.
[58] W. Peiming, A. Andrzej, Computation of dielectric constant of solvent mixtures and electrolyte solutions, Fluid Phase Equilib. 186 (2001) 103–122.
[59] M. Sarmadivaleh, A.Z. Al-Yaseri, S. Iglauer, Influence of temperature and pressure on quartz-water-CO2contact angle and CO2-water interfacial tension, J. Colloid Interface Sci. 441 (2015) 59–64. doi:10.1016/j.jcis.2014.11.010.
[60] Z. Duan, R. Sun, An improved model calculating CO2 solubility in pure water and aqueous NaCl solutions from 273 to 533 K and from 0 to 2000 bar, Chem. Geol. 193 (2003) 257–271. doi:10.1016/S0009-2541(02)00263-2.
[61] M. Ahmad, S. Gersen, Water solubility in CO2 mixtures: Experimental and modelling investigation, in: Energy Procedia, Elsevier, 2014: pp. 2402–2411. doi:10.1016/j.egypro.2014.11.263.

[62] G. Scalabrin, P. Marchi, F. Finezzo, R. Span, A reference multiparameter thermal conductivity equation for carbon dioxide with an optimized functional form, J. Phys. Chem. Ref. Data. 35 (2006) 1549–1575. doi:10.1063/1.2213631.
[63] T.M. Squires, S.R. Quake, Microfluidics: Fluid physics at the nanoliter scale, Rev. Mod. Phys. 77 (2005) 977–1026. doi:10.1103/RevModPhys.77.977.
[64] K. Avila, D. Moxey, A. De Lozar, M. Avila, D. Barkley, B. Hof, The onset of turbulence in pipe flow, Science (80-.). 333 (2011) 192–196. doi:10.1126/science.1203223.
[65] D.C. Venerus, Laminar capillary flow of compressible viscous fluids, J. Fluid Mech. 555 (2006) 59–80. doi:10.1017/S0022112006008755.
[66] L. Chen, Microchannel Flow Dynamics and Heat Transfer of Near-Critical Fluid, Springer Singapore, Singapore, 2017. doi:10.1007/978-981-10-2784-0.
[67] J. Liu, G. Amberg, M. Do-Quang, Numerical simulation of particle formation in the rapid expansion of supercritical solution process, J. Supercrit. Fluids. 95 (2014) 572–587. doi:10.1016/j.supflu.2014.08.033.
[68] B. Weigand, Analytical Methods for Heat Transfer and Fluid Flow Problems, Springer Berlin Heidelberg, Berlin, Heidelberg, 2004. doi:10.1007/978-3-540-68466-4.
[69] A. Günther, K.F. Jensen, Multiphase microfluidics: from flow characteristics to chemical and materials synthesis, Lab Chip. 6 (2006) 1487–1503. doi:10.1039/B609851G.
[70] C. Cai, X. Wang, S. Mao, Y. Kang, Y. Lu, X. Han, W. Liu, Heat transfer characteristics and prediction model of supercritical carbon dioxide (SC-CO2) in a vertical tube, Energies. 10 (2017) 1870. doi:10.3390/en10111870.
[71] G.P. Celata, M. Cumo, V. Marconi, S.J. McPhail, G. Zummo, Microtube liquid single-phase heat transfer in laminar flow, Int. J. Heat Mass Transf. 49 (2006) 3538–3546. doi:10.1016/j.ijheatmasstransfer.2006.03.004.
[72] N.E. Stankova, P.A. Atanasov, R.G. Nikov, R.G. Nikov, N.N. Nedyalkov, T.R. Stoyanchov, N. Fukata, K.N. Kolev, E.I. Valova, J.S. Georgieva, S.A. Armyanov, Optical properties of polydimethylsiloxane (PDMS) during nanosecond laser processing, Appl. Surf. Sci. 374 (2016) 96–103. doi:10.1016/j.apsusc.2015.10.016.
[73] A.K. Goodwin, G.L. Rorrer, Conversion of glucose to hydrogen-rich gas by supercritical water in a microchannel reactor, Ind. Eng. Chem. Res. 47 (2008) 4106–4114. doi:10.1021/ie701725p.
[74] S. Marre, A. Adamo, S. Basak, C. Aymonier, K.F. Jensen, Design and Packaging of Microreactors for High Pressure and High Temperature Applications, Ind. Eng. Chem. Res. 49 (2010) 11310–11320. doi:10.1021/ie101346u.
[75] T. Gothsch, C. Schilcher, C. Richter, S. Beinert, A. Dietzel, S.

Büttgenbach, A. Kwade, High-pressure microfluidic systems (HPMS): flow and cavitation measurements in supported silicon microsystems, Microfluid. Nanofluidics. 18 (2014) 121–130. doi:10.1007/s10404-014-1419-6.
[76] R.M. Tiggelaar, F. Benito-López, D.C. Hermes, H. Rathgen, R.J.M. Egberink, F.G. Mugele, D.N. Reinhoudt, A. van den Berg, W. Verboom, H.J.G.E. Gardeniers, Fabrication, mechanical testing and application of high-pressure glass microreactor chips, Chem. Eng. J. 131 (2007) 163–170. doi:10.1016/j.cej.2006.12.036.
[77] T. Akashi, Y. Yoshimura, Deep reactive ion etching of borosilicate glass using an anodically bonded silicon wafer as an etching mask, J. Micromechanics Microengineering. 16 (2006) 1051–1056. doi:10.1088/0960-1317/16/5/024.
[78] A. Martin, S. Teychené, S. Camy, J. Aubin, Fast and inexpensive method for the fabrication of transparent pressure-resistant microfluidic chips, Microfluid. Nanofluidics. 20 (2016) 92. doi:10.1007/s10404-016-1757-7.
[79] S. Svensson, G. Sharma, S. Ogden, K. Hjort, L. Klintberg, High-pressure peristaltic membrane micropump with temperature control, J. Microelectromechanical Syst. 19 (2010) 1462–1469. doi:10.1109/JMEMS.2010.2076784.
[80] M.F. Ashby, D.R.H. (David R.H. Jones, Engineering materials 1 : an introduction to properties, applications, and design, Butterworth-Heinemann, 2012.
[81] B. Lindroos, A. Lehto, T. Motooka, M. Tilli, Handbook of Silicon Based MEMS Materials and Technologies, William Andrew, 2010.
[82] Y. Takahashi, H. Kondo, H. Niimi, T. Nokuo, T. Suzuki, Fracture strength analysis of single-crystalline silicon cantilevers processed by focused ion beam, Sensors Actuators, A Phys. 206 (2014) 81–87. doi:10.1016/j.sna.2013.11.037.
[83] B.N. Jaya, C. Kirchlechner, G. Dehm, Can microscale fracture tests provide reliable fracture toughness values? A case study in silicon, J. Mater. Res. 30 (2015) 686–698. doi:10.1557/jmr.2015.2.
[84] M. Barlet, J.M. Delaye, T. Charpentier, M. Gennisson, D. Bonamy, T. Rouxel, C.L. Rountree, Hardness and toughness of sodium borosilicate glasses via Vickers's indentations, J. Non. Cryst. Solids. 417–418 (2015) 66–79. doi:10.1016/j.jnoncrysol.2015.02.005.
[85] Ö. Vallin, K. Jonsson, U. Lindberg, Adhesion quantification methods for wafer bonding, Mater. Sci. Eng. R Reports. 50 (2005) 109–165. doi:10.1016/j.mser.2005.07.002.
[86] T. Gupta, Copper interconnect technology, Springer New York, New York, NY, 2009. doi:10.1007/978-1-4419-0076-0.
[87] D.R.F. and M.E. O'Hagan, Measurements of Platinum the Thermal Conductivity and Resistivity from 100 to 900 °C, 1967.
[88] R.M. Tiggelaar, R.G.P. Sanders, A.W. Groenland, J.G.E. Gardeniers, Stability of thin platinum films implemented in high-temperature microdevices, Sensors Actuators, A Phys. 152 (2009) 39–47.

doi:10.1016/j.sna.2009.03.017.
[89] C. Lotter, J.J. Heiland, V. Stein, M. Klimkait, M. Queisser, D. Belder, Evaluation of Pressure Stable Chip-to-Tube Fittings Enabling High-Speed Chip-HPLC with Mass Spectrometric Detection, Anal. Chem. 88 (2016) 7481–7486. doi:10.1021/acs.analchem.6b01907.
[90] A. Note, Agilent Basics of Measuring the Dielectric Properties of Materials, Meas. Tech. 2007 (2005) 32. doi:5989-2589EN.
[91] A.J. Bard, L.R. Faulkner, Electrochemical methods : fundamentals and applications, Wiley, 2001. doi:10.1016/B978-0-08-098353-0.00003-8.
[92] R.. Smith, S.. Lee, H. Komori, K. Arai, Relative permittivity and dielectric relaxation in aqueous alcohol solutions, Fluid Phase Equilib. 144 (1998) 315–322. doi:10.1016/S0378-3812(97)00275-6.

Acta Universitatis Upsaliensis

Digital Comprehensive Summaries of Uppsala Dissertations from the Faculty of Science and Technology 1687

Editor: The Dean of the Faculty of Science and Technology

A doctoral dissertation from the Faculty of Science and Technology, Uppsala University, is usually a summary of a number of papers. A few copies of the complete dissertation are kept at major Swedish research libraries, while the summary alone is distributed internationally through the series Digital Comprehensive Summaries of Uppsala Dissertations from the Faculty of Science and Technology. (Prior to January, 2005, the series was published under the title "Comprehensive Summaries of Uppsala Dissertations from the Faculty of Science and Technology".)

Distribution: publications.uu.se
urn:nbn:se:uu:diva-353964

ACTA
UNIVERSITATIS
UPSALIENSIS
UPPSALA
2018